FULL PAPER

Dalton
www.rsc.org/dalton

The copper(I)/copper(II) transition in complexes with 8-alkylthioquinoline based multidentate ligands †

Cheng-Yong Su,[a] Sen Liao,[a] Matthias Wanner,[b] Jan Fiedler,[c] Cheng Zhang,[a] Bei-Sheng Kang *[a] and Wolfgang Kaim *[b]

[a] *School of Chemistry and Chemical Engineering, Zhongshan University, Guangzhou 510275, P. R. China. E-mail: ceslhq@zsu.edu.cn*

[b] *Institut für Anorganische Chemie, Universität Stuttgart, Pfaffenwaldring 55, D-70569 Stuttgart, Germany. E-mail: kaim@iac.uni-stuttgart.de*

[c] *J. Heyrovsky Institute of Physical Chemistry, Academy of Sciences of the Czech Republic, Dolejškova 3, CZ-18223 Prague, Czech Republic. E-mail: fiedler@jh-inst.cas.cz*

Received 19th August 2002, Accepted 12th November 2002
First published as an Advance Article on the web 13th December 2002

Three linear multidentate ligands incorporating terminal 8-thioquinoline rings and flexible polyethylene glycol or semi-rigid *o*-xylylene spacers have been synthesised: pentadentate 1,5-bis(8-quinolylsulfanyl)-3-oxapentane (OESQ), hexadentate 1,8-bis(8-quinolylsulfanyl)-3,6-dioxaoctane (ODSQ) and tetradentate 1,2-bis(quinolin-8-ylsulfanylmethyl)benzene (OBSQ). Reaction of these ligands with various copper salts afforded three families of copper(I) and copper(II) complexes with the general formula $[Cu(L^1)(L^2)]X_m$: L^1 = OESQ and L^2/X_m = $H_2O/(BF_4^-)_2$ **4**, $DMF/(BF_4^-)_2$ **5**, $H_2O/(ClO_4^-)_2$ **6**, NO_3^-/NO_3^- **7**, NO_3^-/ClO_4^- **8**, none/ BF_4^- **9**; L^1 = ODSQ and L^2/X_m = none/$(BF_4^-)_2$ **10**, none/$(ClO_4^-)_2$ **11**, none/$(NO_3^-)_2$ **12**, none/$Cu(NO_3)_4^{2-}$ **13**, none/ClO_4^- **14**; L^1 = OBSQ and L^2/X_m = ClO_4^-/ClO_4^- **15**, $H_2O/(BF_4^-)_2$ **16**, $DMF/(ClO_4^-)_2$ **17**, $DMF/(BF_4^-)_2$ **18**, NO_3^-/NO_3^- **19**, $H_2O/(NO_3^-)_2$ **20**, $DMSO/(ClO_4^-)_2$ **21**, NO_3^-/BF_4^- **22**, none/BF_4^- **23**. For comparison, three copper complexes $[Cu(EtSQ)_2(ClO_4)_2]$ **1**, $[Cu(EtSQ)_2](ClO_4)$ **2** and $[Cu(MeSQ)_2](ClO_4)$ **3** with the bidentate ligands 8-ethylsulfanylquinoline (EtSQ) and 8-methylsulfanylquinoline (MeSQ) have also been prepared and characterised. The solid-state structures of **1**, **3**, **7**–**9**, **11**, **13**, **18**·CH_3CN, **20**, **21**·CH_3CN, **22** and **23** were determined by X-ray diffraction. Compound **1** shows a distorted octahedral structure with two EtSQ ligands chelating Cu^{2+} in the equatorial plane and two ClO_4^- ions interacting in the axial positions. Compounds **7** and **8** exhibit a similarly distorted coordination environment except that one axial oxygen atom comes from the ligand OESQ and the other from the nitrate anion. The hexadentate ligand ODSQ in compounds **11** and **13** wraps around the central Cu^{2+} ion to form an approximately octahedral geometry resembling that in **1**, however, one sulfur atom must move to the axial position and one ether oxygen atom binds in the equatorial plane. In the four compounds **18**·CH_3CN, **20**, **21**·CH_3CN and **22**, very similar square pyramidal geometries are observed around the central Cu^{2+} ions with four donor atoms from OBSQ occupying three corners of the basal plane and the apical position, the fourth corner being completed by a DMF, H_2O, DMSO or NO_3^- ligand, respectively. In the copper(I) complexes **3**, **9** and **23** the metal centre is distorted tetrahedrally coordinated with two sulfur and two nitrogen donor atoms. The solution structures have been explored by UV–vis and EPR spectroscopy, the copper(II)/copper(I) transition and further reduction processes have been investigated by cyclic voltammetry and UV–vis spectroelectrochemistry. In contrast to the simple 8-alkylthioquinolines MeSQ and EtSQ the bis(NS) ligands allow for a more reversible Cu^I/Cu^{II} transition due to the various effects of steric constraint and additional coordination as provided by the spacers.

Introduction

The very different preferences of copper(I) with its closed-shell d^{10} configuration and copper(II) (d^9, Jahn–Teller situation) in terms of coordination geometries and donor atoms have made it attractive to design and study ligand environments accommodating *both* oxidation states.[1] The Cu^I/Cu^{II} transition has thus been relevant for the problem of reorganisation in electron transfer reactivity (entatic state concept),[2] including the functioning of corresponding proteins.[3] Specifically, it has been essential for the understanding and modeling of mononuclear Type I copper centres and dinuclear Cu_A sites in electron transfer proteins, for which the coordination by imine-N (imidazole nitrogen from histidine), thiolate-S (deprotonated cysteine) and thioether-S (methionine) have been typical.[3]

Recently, a very simple bidentate imine-N/thioether-S ligand, 1-methyl-(2-methylthiomethyl)-1*H*-benzimidazole (mmb),[1c,4] has been shown to accommodate both oxidation states of copper: (i) structural data and DFT calculations have suggested that the Cu^I/Cu^{II} transition of $[Cu^n(mmb)_2]^{n+}$ is based on a rather small structural reorganisation involving mainly the sulfur donors but hardly the nitrogen donor atoms;[1c] (ii) as an interesting consequence, the rare[5] but biochemically relevant[6] phenomenon of valence tautomerism (redox isomerism) equilibria has been observed for systems $(mmb)Cu^I(Q^{-I}) \rightleftharpoons (mmb)Cu^{II}(Q^{-II})$, Q being *o*-quinones.[4]

In this report we shall use another bidentate imine-N/thioether-S component, the 8-alkylthioquinoline function, alone and as part of multidentate ligands. Like mmb, this function can form five-membered chelate rings, however, in comparison to mmb the dialkylthioether has been modified here to an arylalkylthioether, and the imine-N of relatively electron rich benzimidazole has been replaced by a pyridine-type nitrogen donor. In an extension for higher ligand denticity (and steric restriction) *two* such groups were linked by spacers with flexible (OESQ, ODSQ) or semi-rigid backbones (OBSQ), containing no (OBSQ), one (OESQ) or two (ODSQ) additional dialkylether oxygen donor centres for optional coordination.

† Electronic supplementary information (ESI) available. Schemes S1 and S2, Figs. S1–S7, selected bond lengths and angles and preparation of complexes. See http://www.rsc.org/suppdata/dt/b2/b208120m/

DOI: 10.1039/b208120m

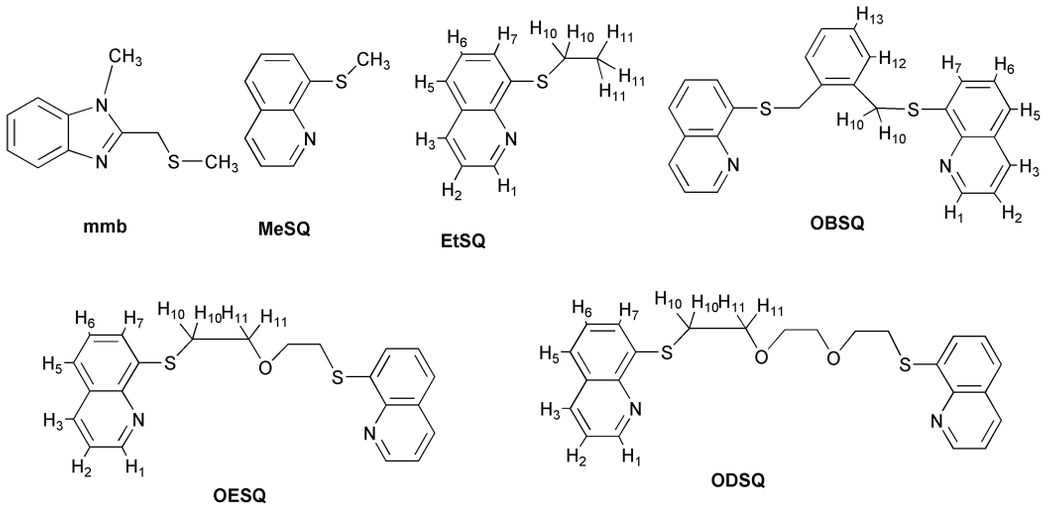

Scheme 1

Results

Syntheses and general characterisation

The compounds 8-methylsulfanylquinoline (MeSQ) and 8-ethylsulfanylquinoline (EtSQ) have been known for some time,[7] however, their transition metal chemistry has not yet been extensively investigated.[8] For instance, no crystal structure related to these two compounds is available in the Cambridge Structural Database. Since methyl and ethyl are not bulky substituents, the coordination mode of these two thioether compounds towards metal ions is expected to be similar to that of quinoline-8-thiolate,[9,10] giving rise to five-membered chelate rings. The three ligands 1,5-bis(8-quinolylsulfanyl)-3-oxapentane (OESQ),[11,12] 1,8-bis(8-quinolylsulfanyl)-3,6-dioxaoctane (ODSQ)[12,13] and 1,2-bis(quinolin-8-ylsulfanylmethyl)benzene (OBSQ) could be prepared in replacement reactions of corresponding dichloro compounds with sodium quinoline-8-thiolate.[10] OESQ and ODSQ contain flexible polyethylene glycol bridges, providing potentially penta- or hexadentate N/S/O mixed donor sets; OBSQ, on the other hand, incorporates a semi-rigid *o*-xylylene backbone, retaining the N_2S_2 tetradentate donor set but imposing some spatial constraint between two terminal 8-alkylthioquinoline groups (Scheme 1). We have previously utilised OESQ and ODSQ to investigate their coordination by some other transition metal centres,[12] and the crystal structure of OBSQ has been reported.[13] In this paper we describe the detailed preparation, purification and characterisation of the three ligands.

The cupric complexes were obtained under ordinary laboratory conditions while the cuprous complexes were handled under an argon atmosphere. Scheme S1 shows the general synthetic route for all complexes, detailed information is given as electronic supplementary information (ESI). The presence of water in the complexes **4**, **6**, **16** and **20** was confirmed by the appearance of a broad band around 3400 cm^{-1} (ν_{O-H}) in their respective IR spectra. Strong absorptions at 1664, 1650 or 1653 cm^{-1} ($\nu_{C=O}$) indicated the existence of DMF in complexes **5**, **17** and **18**. The IR spectra of the complexes containing perchlorate or tetrafluoroborate anions were dominated by the very strong stretching vibrations characteristic of ClO_4^- (1087–1111 and 619–623 cm^{-1}) or BF_4^- (1049–1083 cm^{-1}); in case of **21**, the strong absorption of $\nu_{S=O}$ overlaps with that of ClO_4^-, resulting in an extremely intense band at 1091 cm^{-1}. Information regarding the possible binding modes of nitrate may also be obtained from the IR spectra. In complexes **12** and **20** the single strong bands at 1356 or 1377 cm^{-1} indicate free nitrate groups (D_{3h}); in **8**, **13** and **22**, two intense absorptions associated with asymmetric stretching (C_{2v}) appear at 1435–1469 and 1282–1294 cm^{-1}, suggesting that the NO_3^- groups are coordinated.[14] Similarly, the bands appearing at 1434, 1359, 1293 or 1465, 1347, 1279 cm^{-1} in complexes **7** and **19**, respectively, denote that both free and coordinated NO_3^- groups are present.

In general, both the Cu^{2+} and Cu^+ complexes are air-stable in the solid state, however, their solution stability may vary. The mixing of copper(II) salts with the ligands MeSQ, EtSQ, OESQ or ODSQ in polar solvents such as MeOH, EtOH or DMF leads to typical green solutions which remain unchanged for a long time, suggesting no reduction of the Cu^{2+} ion or oxidation of the ligand by Cu^{2+}. With OBSQ, a yellow Cu^+ complex will appear gradually from the green solution of the Cu^{2+} complex, signifying reduction of Cu^{2+}. Such auto-reduction has been observed before with ligands like 6,6′-dimethyl-2,2′-bipyridine[15] or 2,6-bis(benzimidazol-2′-ylthiomethyl)pyridine.[16] The stabilisation of Cu^+ complexes by S-donor coordination from N_3S- and N_2S_2-type ligands having methyl thioether functions is well known,[17] the propensity of the ligand OBSQ to favour Cu^+ complexes over Cu^{2+} species corresponds to the finding that sterically demanding ligands often stabilise the +1 oxidation state in copper complexes.[18] In any case, all the ligands presented here tolerate both Cu^{2+} and Cu^+.

X-Ray diffraction studies

The molecular structures of the coordination arrangements in compounds **1**, **3**, **7**, **9**, **11**, **13**, **18**·CH_3CN and **23** are depicted in Figs. 1–8, respectively, along with the atom numbering schemes, while the structures of the remaining compounds are given in Figs. S1–S4 of the ESI. Crystallographic information is summarised in Tables 1 and 2 while detailed bond lengths and bond angles are given as ESI.

Copper complexes with bidentate ligands

Crystal structure determination indicates that the coordination sphere around copper(II) in compound **1** is distorted octahedral. The Cu^{2+} ion lies at the crystallographic inversion centre, binding to two EtSQ chelate ligands and two η^1-ClO_4^- anions. Two thioether sulfur atoms, two quinoline nitrogen atoms and two perchlorate oxygen atoms adopt mutual *trans* positions (Fig. 1). The N and S atoms are exactly coplanar. This coordination geometry is quite different from that in complex $[Cu(mmb)_2(\eta^1\text{-}ClO_4)]ClO_4$ with a related imine/thioether chelate ligand (Scheme 1) in which the coordination geometry of pentacoordinate copper(II) falls between the trigonal bipyramidal and square-pyramidal alternatives.[19] However, the N_2S_2 square plane in **1** is reminiscent of that in bis(8-mercaptoquinoline)copper(II),[9] except that the latter is a neutral compound without axial ligands.

Table 1 Crystallographic data for complexes **1**, **2**, **7**–**9** and **11**

	1	**3**	**7**	**8**	**9**	**11**
Formula	$C_{22}H_{22}Cl_2CuN_2O_8S_2$	$C_{20}H_{18}ClCuN_2O_4S_2$	$C_{22}H_{20}CuN_4O_7S_2$	$C_{22}H_{20}ClCuN_3O_8S_2$	$C_{22}H_{20}BCuF_4N_2OS_2$	$C_{24}H_{24}Cl_2CuN_2O_{10}S_2$
M_w	640.98	513.47	580.08	617.52	542.87	699.01
Crystal system	Triclinic	Monoclinic	Triclinic	Triclinic	Triclinic	Monoclinic
Space group	$P\bar{1}$	$C2/c$	$P\bar{1}$	$P\bar{1}$	$P\bar{1}$	$C2/c$
a/Å	7.863(3)	12.3793(19)	8.136(4)	8.232(1)	10.8405(2)	12.929(2)
b/Å	8.983(2)	12.872(2)	12.159(8)	12.670(2)	10.9739(2)	17.733(2)
c/Å	9.942(2)	14.528(3)	12.858(7)	13.103(2)	11.4155(2)	24.425(2)
α/°	66.95(2)	90	99.87(1)	73.69(1)	66.180(1)	90
β/°	87.32(2)	113.533(12)	106.50(1)	73.39(1)	72.658(1)	98.72(1)
γ/°	79.51(2)	90	104.65(1)	73.28(1)	69.596(1)	90
V/Å^3	635.1(3)	2122.3(6)	1138.7(11)	1224.5(3)	1144.64(4)	5535.2(12)
Z	1	4	2	2	2	8
D_c/g cm^{-3}	1.676	1.607	1.692	1.675	1.575	1.678
μ/mm^{-1}	1.286	1.382	1.197	1.226	1.1870	1.193
T/K	173	173	293	293	293	293
R^a	0.0406	0.0327	0.0547	0.0672	0.0775	0.0422
wR^b	0.0970	0.0852	0.1219	0.1711	0.2279	0.1074

^{a} $R = = \Sigma(|F_o| - |F_c|)/\Sigma|F_o|$ ^{b} $wR = [(\Sigma w(F_o^2 - F_c^2)^2/\Sigma w(F_o^2)^2)^{1/2}$.

Table 2 Crystallographic data for complexes **13**, **18**·CH_3CN, **20**, **21**·CH_3CN, **22** and **23**

	13	**18**·CH_3CN	**20**	**21**·CH_3CN	**22**	**23**
Formula	$C_{24}H_{24}CuN_6O_{14}S_2$	$C_{31}H_{30}Cl_2CuN_4O_9S_2$	$C_{26}H_{22}CuN_4O_7S_2$	$C_{30}H_{29}Cl_2CuN_3O_9S_3$	$C_{26}H_{20}BCuF_4N_3O_3S_2$	$C_{26}H_{20}BCuF_4N_2S_2$
M_w	811.69	801.15	630.14	806.18	636.92	574.91
Crystal system	Monoclinic	Monoclinic	Monoclinic	Triclinic	Triclinic	Orthohombic
Space group	$P2_1/c$	$P2_1/c$	$P2_1/c$	$P\bar{1}$	$P\bar{1}$	$Pna2_1$
a/Å	15.429(2)	12.066(6)	11.481(2)	7.8552(10)	7.894(1)	15.120(2)
b/Å	9.924(2)	13.164(26	14.804(2)	13.429(2)	11.4168(14)	8.363(1)
c/Å	20.516(3)	21.395(12)	15.622(2)	16.843(2)	15.9474(19)	19.421(2)
α/°	90	90	90	85.358(2)	105.433(2)	90
β/°	102.697(9)	93.82(4)	93.51(1)	88.564(2)	92.278(2)	90
γ/°	90	90	90	78.686(2)	104.610(2)	90
V/Å^3	3064.5(8)	3391(3)	2650.2(7)	1736.4(4)	1331.8(3)	2455.8(5)
Z	4	4	4	2	2	4
D_c/g cm^{-3}	1.759	1.569	1.579	1.542	1.588	1.555
μ/mm^{-1}	1.604	0.985	1.036	1.019	1.040	1.109
T/K	294	173	296	293	293	293
R^a	0.0310	0.0582	0.0539	0.0642	0.0535	0.0622
wR^b	0.0537	0.1340	0.1076	0.1720	0.1402	0.1606

^{a} $R = = \Sigma(|F_o| - |F_c|)/\Sigma|F_o|$ ^{b} $wR = [(\Sigma w(F_o^2 - F_c^2)^2/\Sigma w(F_o^2)^2)^{1/2}$.

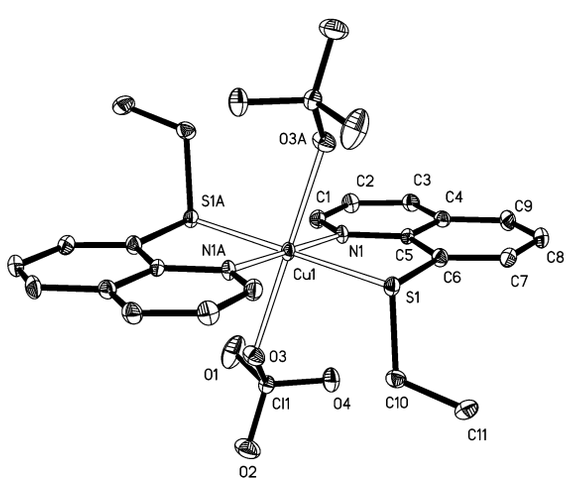

Fig. 1 Molecular structure and atom labeling of complex **1**, $[Cu(EtSQ)_2(ClO_4)_2]$.

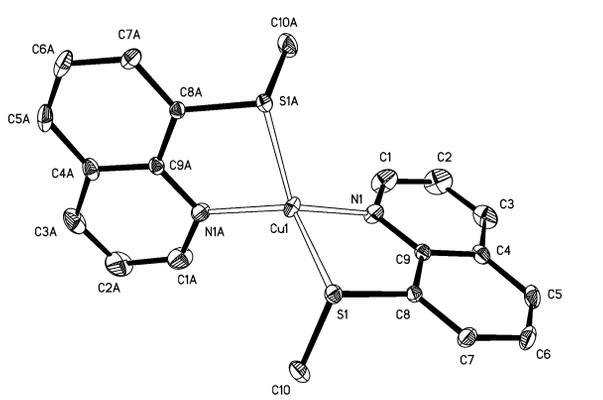

Fig. 2 Molecular structure and atom labeling of the $[Cu(MeSQ)_2]^+$ cation in complex **3**.

In contrast, the Cu^+ ion in compound **3** is tetracoordinated to two sulfur atoms and two nitrogen atoms from two C_2 symmetry-related MeSQ ligands, providing a distorted tetrahedral geometry which is typical for many Cu^+ complexes with sulfur donor atoms (Fig. 2);[20] some examples with coordination numbers five or three have also been reported.[16,21] The small bite angle N(1)–Cu–S(1) of 87.21° imposed by the five-membered chelating ring causes a pronounced deviation from the regular tetrahedron, the largest angle is found for N(1)–Cu–N(1A) at 131.82°. However, this is still significantly different from the analogous $[Cu(mmb)_2]BF_4$ in which the N–Cu–N angle is close to linear (169.75°).[1c]

Copper(II) complexes with pentadentae OESQ

The structural analyses of **7** and **8** reveal a complex cation $[Cu(OESQ)(NO_3)]^+$ with different counter ions NO_3^- and

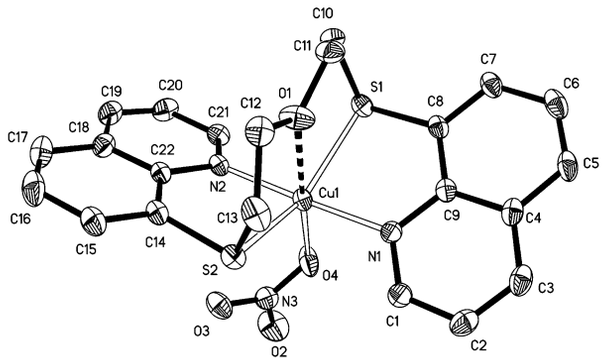

Fig. 3 Molecular structure and atom labeling of the $[Cu(OESQ)(NO_3)]^+$ cation in complex **7**.

ClO_4^-, respectively (Fig. 3 and Fig. S1 of ESI). Obviously, the NO_3^- anion is preferred over ClO_4^- to enter the coordination sphere of Cu^{2+}, and the complete six-coordinate environment is little influenced by the counter ions. The two 8-alkylthioquinoline rings adopt a *trans* configuration to chelate the central Cu^{2+} ion with dihedral angles of 48.0° (**7**) or 52.6° (**8**), resulting in mean deviations of about 0.33 Å from the best plane for four equatorially coordinated atoms. The diethylene glycol bridge strides diagonally over the equatorial plane, leaving the ether oxygen weakly coordinated at the apical position. The opposite apical position is occupied by one oxygen atom from the nitrate group. Thus, the Cu^{2+} ions are in a distorted octahedral coordination geometry. The N–Cu–N and O–Cu–O angles are close to 180°, but the S–Cu–S angles deviate by about 33° from the linear geometry. This is mainly because of the short diethylene glycol "strap" with quite elongated Cu–O distances (2.446 and 2.519 Å for **7** and **8**, respectively). The much shorter Cu–O distances (2.113 and 2.128 Å) to the other axial oxygen atom of anionic NO_3^- appear to stabilise this coordination, excluding any other interactions e.g. with solvent molecules. Only a few Cu^{2+} complexes with ligands containing N_2S_2O donor sets were reported in the literature.[22] Two of them show very similar coordination environments, $[Cu(OdtoxH)](ClO_4)\cdot[Cu(OdtoxH_2)](ClO_4)$ (Odtoxh = 7-oxa-4,10-dithiatridecane-2,12-dione dioxime)[22a] and $[Cu(L)(ClO_4)]ClO_4$ (L = 1,9-bis(2-pyridyl)-5-oxa-2,8-dithianonane)[22b] while all others involve macrocyclic compounds with very different donor arrangements. The structure (Fig. 4) of complex $[Cu(OESQ)]BF_4$ (**9**) with tetracoordinate copper(I) is discussed further below.

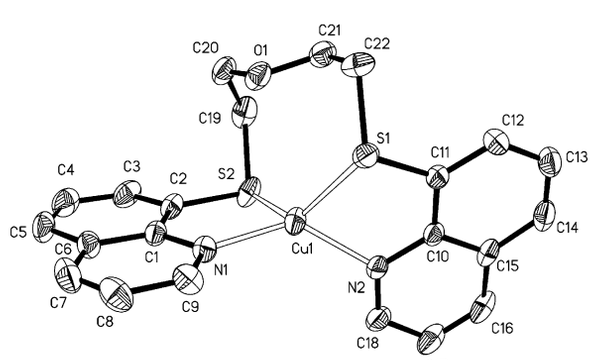

Fig. 4 Molecular structure and atom labeling of the $[Cu(OESQ)]^+$ cation in complex **9**.

Copper(II) complexes of hexadentate ODSQ

Compared with OESQ, the ligand ODSQ contains a longer triethylene glycol spacer between two terminal 8-alkylthioquinoline rings, providing six potential donors ($N_2S_2O_2$). The flexible bridge facilitates this potentially hexadentate ligand to wrap around a Cu^{2+} ion, occupying all six coordinations sites to lead to the quite distorted octahedral $[Cu(ODSQ)]^{2+}$ cation in **11** and **13** (Figs. 5 and 6).

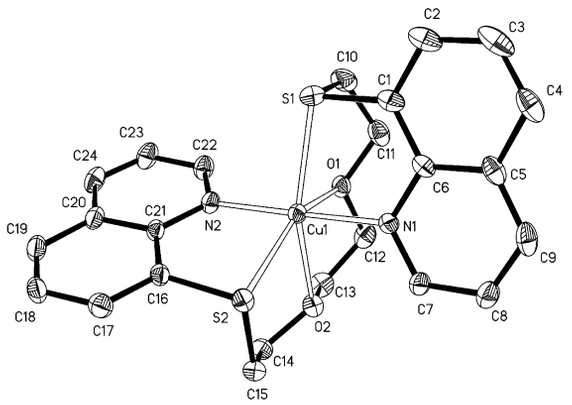

Fig. 5 Molecular structure and atom labeling of the $[Cu(ODSQ)]^{2+}$ dication in complex **11**.

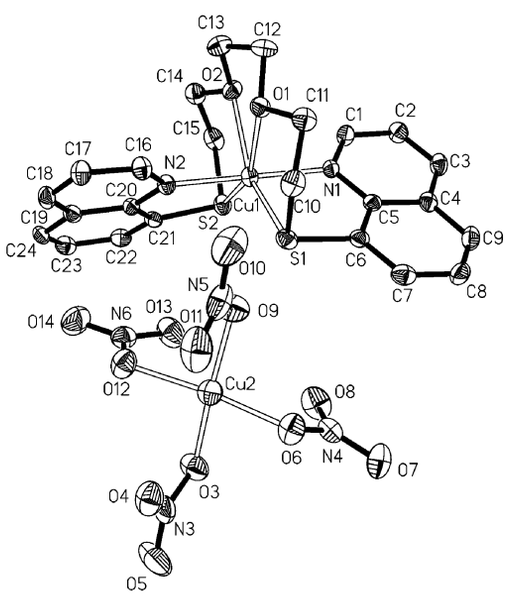

Fig. 6 Molecular structure and atom labeling of the $[Cu(ODSQ)]^{2+}$ dication and the $[Cu(NO_3)_4]^{2-}$ dianion in complex **13**.

The difference from the geometry in **7** and **8** is that one sulfur atom moves to the "apical" position (elongated octahedral model) and one of the ether oxygen atoms occupies an equatorial site to form the equatorial plane with another sulfur atom and two quinoline nitrogen atoms. This arrangement is enforced because the two ether oxygen atoms are separated only by an ethylene bridge and must be in *cis* position. The resulting five contiguous five-membered chelating rings then lead to two sulfur atoms in *cis* position as well. Therefore, two 8-alkylthioquinoline rings adopt dihedral angles of 65.0 and 65.5° in **11** and **13**, respectively, while the two nitrogen atoms in *trans* position retain a nearly linear N–Cu–N angle. The four equatorial donors N_2SO are not planar as those in **7** and **8** with average displacements of 0.31 and 0.27 Å from the mean plane in **11** and **13**, respectively. This may be caused by the slightly larger O(1)–Cu–S(2) angles (149.8 and 152.9°) as compared with the S–Cu–S angles in **7** and **8**. However, the axial O(2)–Cu–S(1) angles (151.09 and 151.9°) are remarkably smaller than 180°. At 130.1 and 127.6° in **11** and **13**, the S–Cu–S angles are very much larger than the 90° required for ideal octahedral geometry, implying the possibility for solvent molecules to interact with

the Cu^{2+} ion between these Cu–S bonds. Some other ligands with $N_2S_2O_2$ donor sets have been reported,[20c,22d,23] and similar coordination environments have been found for Cu^{2+} complexes[23a–c,24] but no structure showed the same donor atom arrangement like the ODSQ system. Another noticeable feature is that one $[Cu(\eta^1\text{-}NO_3)_4]^{2-}$ planar coordination motif was formed in **13** to act as one counter-anion instead of two NO_3^- anions in **12**. This suggests that the flexible ODSQ ligand has a preference to embrace one Cu^{2+} ion to form a mononuclear complex rather than bridge two or more Cu^{2+} ions to give polynuclear complexes, in contrast to the coordination behaviour of silver(I).[12a,b]

Copper(II) complexes of tetradentate OBSQ

As shown in Fig. 7 and Figs. S2–S4 of the ESI completely different coordination geometries are formed for the Cu^{2+} ions in complexes $[Cu(OBSQ)L^2]^{n+}$.

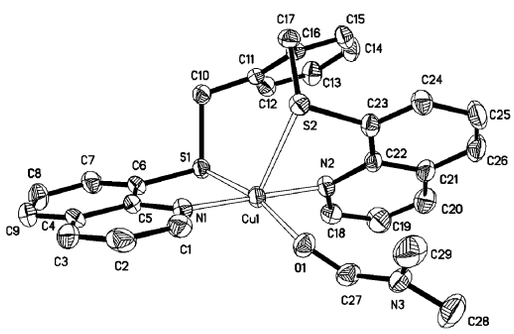

Fig. 7 Molecular structure and atom labeling of the $[Cu(OBSQ)(DMF)]^{2+}$ dication in complex **18**.

The arrangements may be best described as distorted square-pyramidal. The semi-rigid *o*-xylylene bridge is too short to allow the two 8-alkylthioquinoline rings to form an equatorial plane in *trans* configuration like that in the above complexes. Alternatively, one sulfur atom is drawn back to an apical position, leaving two nitrogen atoms and one sulfur centre in the basal plane. The remaining corner is then occupied by a small molecule like DMF, H_2O, DMSO or NO_3^- in the complexes **18**·CH_3CN, **20**, **21**·CH_3CN and **22**, respectively. The CH_3CN solvent molecules are located in the crystal lattice but do not participate in metal coordination. It is interesting to note that the N–Cu–N angles retain an almost linear *trans* position in all the structures. The two 8-alkylthioquinoline rings are rotated around the N–Cu–N axis to give dihedral angles of 49.2, 54.5, 46.0 and 45.3°, respectively; the deviations of the Cu^{2+} ions from the mean basal planes are 0.14, 0.31, 0.19 and 0.22 Å in the cationic complex $[Cu(OBSQ)L^2]$, L^2 = DMF, H_2O, DMSO and NO_3^-, respectively. The square-pyramidal geometries of these complexes can also be confirmed and quantified by the analysis of their angular structural parameters $\tau = (\beta - \alpha)/60°$, where τ is the index of trigonality and α and β are the basal angles. For the ideal square-pyramid $\tau = 0$ while $\tau = 1$ for the ideal trigonal bipyramid.[25] The low values of 0.22, 0.35, 0.27 and 0.31 for **18**·CH_3CN, **20**, **21**·CH_3CN and **22**, respectively, indicate some moderate distortions from the ideal square pyramidal geometry, in the same order as the out-of-plane displacement values discussed above. The main reason to cause such a distortion is the spatial constraint imposed by the *o*-xylylene spacer fragment. As it connects two 8-alkylthioquinoline groups without providing any donor atoms, the seven-membered chelating rings formed with Cu^{2+} ions result in expanded S–Cu–S angles of 109.6–116.7°. Moreover, careful analysis of the crystal structures indicate that secondary interactions between Cu^{2+} ions and the oxygen containing anions or solvent molecules below the basal plane are present for all the complexes. These Cu ··· O interaction distances lie in the range of 2.62–2.90 Å, suggesting that the counter ions or solvent molecules associate with the central Cu^{2+} ions in solution. Structures of copper complexes with ligands incorporating N_2S_2 donor sets are much more common than those with N_2S_2O or $N_2S_2O_2$ donor sets because they represent typical models to mimic the inorganic "type 1" sites of blue copper proteins.[1c,20c–e,25,26] However, some of these proteins like azurin exhibit an N_2S_2O donor arrangement with very weakly bonded O donors (Cu ··· O > 3.0 Å).[27]

Copper(I) complexes with tetradentate OESQ and OBSQ

The coordination geometries of the Cu^+ complexes with the ligands OESQ (**9**) (Fig. 4) and OBSQ (**23**) (Fig. 8) show little difference when compared with **3**.

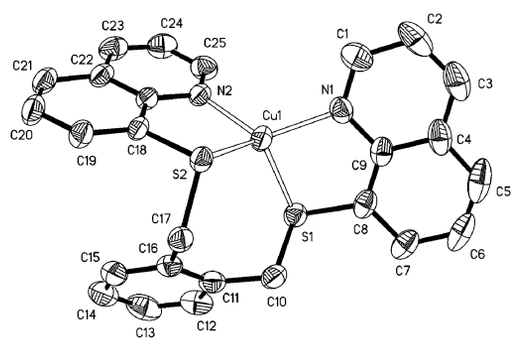

Fig. 8 Molecular structure and atom labeling of the $[Cu(OBSQ)]^+$ cation in complex **23**.

Two sulfur and two nitrogen atoms are bonded to Cu^+, and the small bite angles N–Cu–S from the chelating 8-alkylthioquinoline groups (84.1–88.1°) lead to a pronounced deviation from the tetrahedral angle. The largest angle remains N(1)–Cu–N(1A) at 134.8° in **9** while the S–Cu–S angle increases to 128.8° because of the diethylene glycol spacer. In **23** the S–Cu–S angle at 112.3° closely resembles those in Cu^{2+} complexes such as **18**·CH_3CN, **20**, **21** or **22**, suggesting at first a small reorganisation for the transition between both copper oxidation states. However, the N–Cu–N angle at 122.8° in **23** is rather small, especially when compared to the *ca.* 175° in corresponding Cu^{2+} systems.

General structure discussion

In all Cu^{2+} complexes the two quinoline nitrogen atoms adopt a *trans* position with the N–Cu–N angles close to 180°. The terminal quinoline rings may then rotate along this axis to accommodate variable S–Cu–S angles, moving one of two sulfur atoms from an equatoral position to an apical site. Such spatial requirements are related to the length and flexibility of the bridges between the two 8-alkylthioquinoline groups. In the case of EtSQ, two 8-alkylthioquinoline groups are completely free to adopt a coplanar *trans* conformation, giving the most regular geometry in **1**. The coordination geometries at the Cu^{2+} centres may vary between different degrees of distortion of an octahedron; a distorted square pyramid is observed with the OBSQ ligand. The Cu^+ ions are always coordinated in a distorted tetrahedral fashion. The different bridges between two quinoline rings affect the bond angles but are flexible enough to fit the distorted tetrahedral environment.

The Cu–N distances of the Cu^{2+} complexes range between 1.966 and 2.024 Å and those of the Cu^+ complexes between 1.994 and 2.021 Å. These distances are normal when compared with Cu–N bond distances found in other copper complexes with N-heterocyclic ligands such as pyridines, imidazoles or benzimidazoles.[23–26,28] Remarkably, there is little difference

Table 3 EPR and UV–vis spectral data for complexes in DMF

Compound	EPR [a]				UV–vis
	$g_{\|\|}$	$A_{\|\|}$	$g_{\perp}$	$g_{\|\|}/A_{\|\|}$	λ_{max} (ε) [b]
Cu^{2+} complexes					
$[Cu(EtSQ)_2](ClO_4)_2$, **1**	2.393	133	2.084	180	793 (35)
$[Cu(OESQ)(H_2O)](BF_4)_2$, **4**	2.396	143	2.080	167	754 (123)
$[Cu(OESQ)(DMF)](BF_4)_2$, **5**	2.398	147	2.082	164	752 (204)
$[Cu(OESQ)(H_2O)](ClO_4)_2$, **6** [c]	2.396	143	2.080	167	752 (157)
$[Cu(OESQ)(NO_3)]ClO_4$, **8**	2.401	138	2.081	174	754 (226)
$[Cu(OESQ)(NO_3)]NO_3$, **7**	n.d.	n.d.	n.d.	n.d.	758 (195)
$[Cu(ODSQ)](BF_4)_2$, **10**	2.399	138	[c]	174	756 (111)
	2.209	139	[c]	159	839 (110)
$[Cu(ODSQ)](ClO_4)_2$, **11**	2.397	137	[c]	176	755 (105)
	2.210	141	[c]	156	832 (104)
$[Cu(ODSQ)](NO_3)_2$, **12**	2.396	134	[c]	178	756 (113)
	2.211	142	[c]	155	838 (110)
$[Cu(ODSQ)][Cu(NO_3)_4]$, **13**	n.d.	n.d.	n.d.	n.d.	759 (191)
					840 (185)
Cu^{+} complexes					
$[Cu(EtSQ)_2]ClO_4$, **2**	—	—	—	—	369 (3400)
$[Cu(MeSQ)_2]ClO_4$, **3**	—	—	—	—	359 (6080)
$[Cu(OESQ)]BF_4$, **9**	—	—	—	—	375 (5836)
$[Cu(ODSQ)]ClO_4$, **14**	—	—	—	—	368 (4823)

[a] g factor components determined at 110 K in glassy frozen solution; $A_{||}$ in units of 10^{-4} cm^{-1}. [b] Wavelengths in nm, molar absorption coefficients in dm^3 mol^{-1} cm^{-1}. [c] Not resolved because of signal overlap.

between the Cu^{2+} and Cu^{+} species. By contrast, the Cu–S distances vary quite a bit, depending on the coordination geometries and oxidation states of the copper atoms. For six-coordinate complexes, the Cu^{II}–S distances range between 2.39 and 2.43 Å with the axial distances being slightly longer than the equatorial ones. For the five-coordinate complexes, the difference becomes even more significant: The in-plane Cu–S bonds range between 2.326 and 2.376 Å while the apical Cu–S distances are found between 2.514 and 2.616 Å. The in-plane bonds of the square-pyramidal complexes show slightly shorter distances than the equatorial bonds of elongated octahedral complexes while the axial bonds differ much more.

The Cu^{I}–S distances lie in the range from 2.28 to 2.40 Å, *i.e.* somewhat shorter than the Cu^{II}–S distances. The axial Cu–O distances (2.425 Å) in complex **1** are at the shorter end of the range (2.38–2.70 Å) found for axial Cu–ClO_4^- interactions in six-coordinate Cu^{2+} complexes.[28] By contrast, the axial Cu–O bonds in **7** and **8** are unsymmetrical: one is distinctly shortened at 2.113 or 2.128 Å while the other is substantially elongated at 2.466 or 2.519 Å, respectively. The equatorial Cu–O bond distances (2.128 and 2.519 Å) in "octahedral" **11** and **13** are shorter than the axial ones (2.389 and 2.306 Å) but still markedly longer than the in-plane Cu–O bond distances of square-pyramidal complexes (2.021–2.087 Å). The shortest Cu–O bond distances were found for the planar $[Cu(NO_3)_4]^{2-}$ dianion in **8**, ranging between 1.957 and 1.980 Å.

UV–Vis absorption spectroscopy

The absorption maxima and molar absorption coefficients for the complexes of MeSQ, EtSQ, OESQ and ODSQ are listed in Table 3, for complexes of OBSQ they are summarised in Table 4. Fig. S5 (ESI) shows absorption spectra for **1**, **5**, **11** and **21** in DMF solution, representing typical d–d transition patterns of Cu^{2+} complexes. Although it is difficult to predict solution structures of the Cu^{2+} complexes from electronic spectroscopy alone because of a wide range of possible geometrical distortions and the typically poor resolution of absorption bands,[29] some structural information is available by careful comparison of different kinds of complexes with the support of solid state structures. One broad, unsymmetrical band was found for complex $[Cu(EtSQ)_2(ClO_4)_2]$ **1** with a maximum at 793 nm, indicative of a weak field and relatively high symmetry (Fig. S5). The slope extending till the near infrared region suggests a splitting of the t_{2g} and e_g levels which seems difficult to resolve. The absorption patterns of the OESQ complexes are quite similar to that of **1**, except that the λ_{max} value is slightly blue-shifted and the intensity increased. This is reasonable because of unsymmetrical axial bonding. In solution, the axial interactions may be weakened even further due to ligand constraints and solvent exchange.[30] Elongation of the axial bonds may shift the $d_{xy} \longrightarrow d_{(x^2-y^2)}$ and $d_{xy,yz} \longrightarrow d_{(x^2-y^2)}$ transitions to higher energy and make the Cu^{2+} ion more positive to bind the equatorial donors more strongly.[29,31] The complexes with the potentially hexadentate ODSQ display even broader, unsymmetrical bands with two discernible adjacent maxima at about the same position as in the OESQ complexes. The shape of the absorption suggests that more than one Cu^{2+} species may exist in the solution (*cf.* EPR section). In contrast to the OESQ complexes, the short axial bonds in the ODSQ complexes may be responsible for the additional lower-energy band. On the other hand, the ligand ODSQ may relax in solution under competition from the solvent molecules (DMF) which may bind between the two S–Cu bonds as discussed above. Therefore, an axially lengthened species may result in a higher-energy band. This assumption of two coexisting species with somewhat different coordination geometries is confirmed by EPR spectroscopy as discussed later. In any case, the relatively low energies of the absorption maxima for the above species are indicative of weak crystal fields with the equatorial donors in a distorted square arrangement. By contrast, all five-coordinate complexes with the pentadentate OBSQ display two separate bands in the visible spectra with the intensity of the higher-energy band being markedly higher than the intensity of the lower-energy band (Fig. S5, ESI). Such a pattern is characteristic for distorted square-pyramidal Cu^{2+} complexes, in contrast to the trigonal-bipyramidal geometry where the opposite intensity ratio is typical.[29] This finding suggests that the overall square-pyramidal coordination environment found in the solids is retained in solution. Similar spectra were reported for a number of other square-pyramidal Cu^{2+} complexes.[29,32] All Cu^{+} complexes exhibit a moderately intense band in the range between 359 and 380 nm which may be assigned to metal-to-ligand charge-transfer (MLCT) transitions.[20f,33]

Table 4 EPR and UV–vis spectral data for complexes of OBSQ

Compound	EPR [a]							UV (ε) [b]
	DMF [c]			CH_2Cl_2				DMF
	$G_{\|\|}$	$A_{\|\|}$	$g_{\|\|}/A_{\|\|}$	$g_{\|\|}$	$A_{\|\|}$	$g_\perp$	$g_{\|\|}/A_{\|\|}$	λ_{max} (ε) [b]
$[Cu(OBSQ)(ClO_4)]ClO_4$, **15**	2.390	135	177	2.239	148	2.069	151	639 (132)
	2.231	152	147					954 (75)
$[Cu(OBSQ)(H_2O)](BF_4)_2$, **16**	2.396	138	174	2.210	144	2.061	153	641 (91)
	2.232	152	147					939 (53)
$[Cu(OBSQ)(DMF)](BF_4)_2$, **18** [d]	2.395	136	176	2.229	152	2.086	147	636 (94)
	2.232	152	147					937 (57)
$[Cu(OBSQ)(DMSO)](BF_4)_2$, **21**	2.395	136	176	2.232	152	2.075	147	644 (128)
	2.232	152	147					937 (77)
$[Cu(OBSQ)(NO_3)]NO_3$, **19**	2.398	135	177	n.d.	n.d.	n.d.	n.d.	648 (133)
	2.234	152	147					938 (99)
$[Cu(OBSQ)(NO_3)]BF_4$, **22**	2.403	136	176	n.d.	n.d.	n.d.	n.d.	645 (135)
	2.252	148	152					943 (93)
$[Cu(OBSQ)(DMF)](ClO_4)_2$, **17**	n.d.	n.d.	n.d.	n.d.	n.d.	n.d.	n.d.	638 (114)
								938(69)
$[Cu(OBSQ)]BF_4$, **23**	—	—	—	—	—	—	—	380 (5890)

[a] *g* factor components determined at 110 K in glassy frozen solution; $A_{||}$ in units of 10^{-4} cm^{-1}. [b] Wavelengths in nm, molar absorption coefficients in dm^3 mol^{-1} cm^{-1}. [c] $g_\perp$ not resolved because of signal overlap. [d] *g* factor components for **18** in CH_2Cl_2 were obtained from *in situ* electrolytic oxidation of **23** due to the low solubility of **18** in CH_2Cl_2.

Electron paramagnetic resonance

Representative EPR spectra of Cu^{2+} complexes with the ligands EtSQ, OESQ, ODSQ and OBSQ are shown in Fig. 9, and the

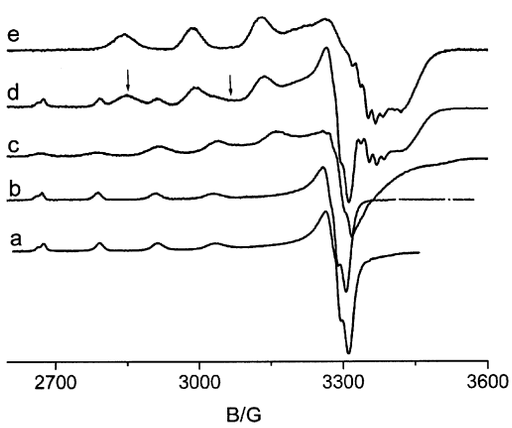

Fig. 9 X-Band EPR spectra of (a) complex **4** in DMF, (b) complex **1** in DMF, (c) complex **10** in DMF, (d) complex **15** in DMF and (e) complex **15** in CH_2Cl_2, each at 110 K. Arrows on curve (d) indicate the positions to determine the *g* components for two sets of signals.

spectral data are listed in Tables 3 and 4. The spectra of all complexes as measured in frozen DMF solution are axial with $g_{||} > g_\perp > 2.0$, indicating a $d_{x^2-y^2}$ ground state[34] which is in agreement with the electronic spectroscopy assignments. However, some differences are obvious between complexes of different ligands. The spectrum of **1** shows the typical four-line hyperfine splitting $A_{||}$ with the signals pertaining to ^{63}Cu and ^{65}Cu slightly resolved at the low-field component. The most remarkable feature is that the $g_{||}$ value of 2.393 is substantially higher than that of the majority of known Cu^{2+} complexes incorporating sulfur donors.[12,23b,25,33–35] Such high values are well known to occur with ligands containing hard donors like oxygen,[36] but rarely with sulfur donor ligands.[37] A factor potentially contributing to an increase of $g_{||}$ is the distortion from square-planar geometry to a rhomboid (diamond) shape.[38] In contrast, low $g_{||}$ values are common for six-coordinate Cu^{2+} complexes with equatorial N_2S_2 donor sets.[20a,f,23a,39] More evidently, the complexes $[Cu(OESQ)L^2]^{n+}$ also display EPR spectra with high $g_{||}$. Referring to their solid state structures in which the equatorial S–Cu–S angles are far from linear, a distortion of the square-planar geometry may not be unexpected for their solution structure. The degree of geometrical distortion had been approached by a parameter $g_{||}/A_{||}$ ($A_{||}$ in cm^{-1}) with values less than 140 associated with square-planar structures whereas higher values indicate marked distortions towards a tetrahedron.[38,40] For the OESQ complexes, the $g_{||}/A_{||}$ ratios fall in the range from 164 to 180, in agreement with significant deviation from planarity. Together with the high $g_{||}$ values, these parameters suggest weak fields with some tetrahedral distortion,[32b,41] consistent with the results from electronic spectroscopy.

EPR spectra of the complexes with the ODSQ ligand showed some complexity in both the $g_{||}$ and $g_\perp$ regions. Obviously there are two different species. The minor component exhibits spectra like those of EtSQ and OESQ complexes while the major species shows significantly smaller $g_{||}$ and slightly larger $A_{||}$ values. The relatively lower $g_{||}/A_{||}$ ratios of about 155–159 for the main species indicate a moderate distortion from planarity, less than that of the minor species. This finding is in good agreement with the results from electronic spectroscopy.

The presence of two species becomes even more clear in the EPR spectra of the OBSQ complexes. A very small set of signals overlapping with the main spectrum can be completely resolved. The $g_{||}$ values of the main species are slightly higher than those of the major species in ODSQ complexes, and the $A_{||}$ values have increased remarkably. Therefore, the $g_{||}/A_{||}$ ratios fall in the range between 147 and 152, signifing relatively small structural distortion. It is interesting to note that the complexes of OBSQ display solely one species in CH_2Cl_2 solution, closely similar to the main signals in DMF. This finding confirms the previous suggestion of two species in DMF, indicating the crucial influence of the solvent on the solution structures. Similar observations of more than one Cu^{2+} species by EPR have been reported.[37d,41a,42] By contrast, the electronic spectra of the OBSQ complexes showed no clear resolution of two species in DMF solution like the ODSQ complexes. This may be understandable because the minor species of the former is much less abundant and tetrahedral distortion normally results in a weak field with lower intensity of the absorption band.[29]

Cyclic voltammetry

The electrochemistry of the complexes was investigated by cyclic voltammetry in DMF and dichloromethane solutions. Poor solubility in the latter solvent precluded measurements of complexes with the ODSQ ligand. The electrochemical

response of the complexes was complicated by adsorption of the reduction products at the electrode surface, especially at the platinum working electrode. The potentials and currents of adsorption peaks depend strongly on the experimental conditions, therefore, a careful choice of optimal parameters was necessary to minimise such effects. Cyclic voltammograms of the complexes **6**, **15** and **11** are depicted in Figs. 10 and Fig. S6

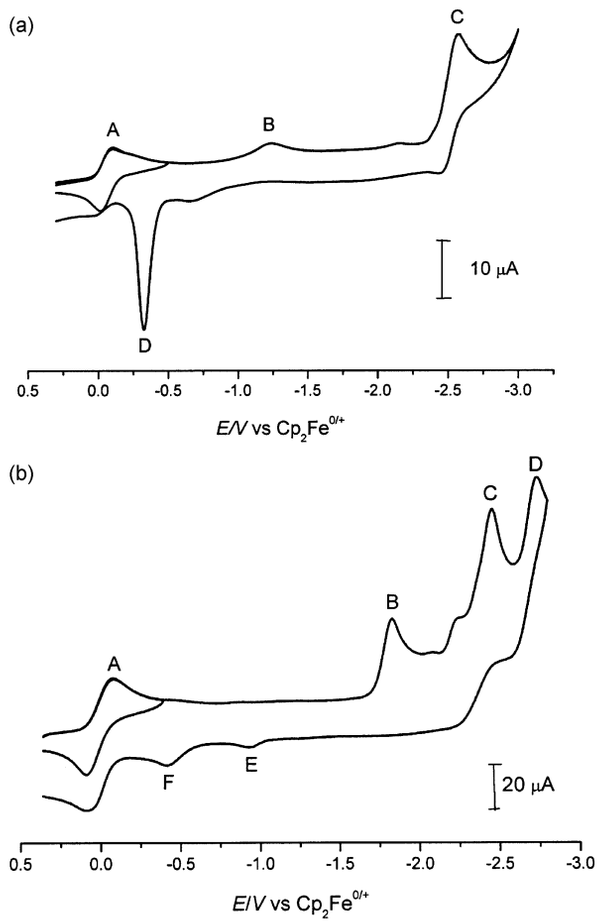

Fig. 10 Cyclic voltammograms of compounds (a) **6**, using a platinum working electrode and (b) **15**, using a glassy carbon working electrode, each in DMF/0.1 mol dm^{-3} Bu_4NPF_6 at 100 mV s^{-1} scan rate.

(ESI), representing the general electrochemical behaviour of complexes with the ligands OESQ, ODSQ and OBSQ, respectively. More information is available in Tables 5 and 6.

The redox behaviour of all complexes with the ligands OESQ and ODSQ are quite similar, showing three principal redox processes in DMF solution, except for **13**. As listed in Table 5, the

Table 5 Cyclic voltammetry data for complexes of the ligands MeSQ, EtSQ, OESQ and ODSQ[a]

	DMF[b]				CH_2Cl_2[c]	
Compound	$E_{1/2}$[d]	E_{pc}[e]	E_{pc}[f]	E_{pa}[f]	$E_{1/2}$[d]	E_{pc}[e]
1	—[g]	−1.11	−2.62	−2.42	0.48	−1.74
4	−0.03	−1.23	−2.51	−2.36	0.31	−1.67
5	−0.01	−1.24	−2.52	−2.47	0.27	−1.68
6	−0.05	−1.20	−2.54	−2.42	0.26	−1.63
7	−0.01	−1.30	−2.63	−2.39	0.15	−1.67
10	−0.06	−1.17	−2.48	−2.31	0.07	−1.71
11	−0.04	−1.20	−2.50	−2.34	0.06	−1.68
12	−0.07	−1.20	−2.53	−2.35	n.d.	n.d.
13	−0.03	−1.12	−2.51	−2.33	n.d.	n.d.
	−0.62[h]					

[a] Potentials in V *vs.* ferrocenium–ferrocene, 0.1 M Bu_4NPF_6 solution, scan rate 100 mV s^{-1}. [b] With platinum working electrode. [c] With glassy carbon working electrode. [d] Half-wave potentials for the couple $[Cu^{II}L]^{2+}/[Cu^{I}L]^{+}$. [e] Cathodic peak potential for irreversible $[Cu^{I}L]^{+}/Cu^{0}$ reduction step. [f] Cathodic and anodic potentials for quasireversible L/L^{-} reduction step; n.d. = not measured due to poor solubility. [g] Irreversible, $E_{pc} = -0.28$, $E_{pa} = 0.10$ V. [h] Half-wave potentials due to the Cu^{2+}/Cu^{+} couple of $[Cu(NO_3)_4]^{2-}$.

first reversible process (A) with half-wave potentials appearing between −0.01 and −0.07 V *vs.* ferrocene (Fc^{+}/Fc) is attributed to the Cu^{2+}/Cu^{+} one-electron transfer. The following cathodic peak (B) without return counterpeak but resulting in a large desorption peak in the reverse scan is assigned to the irreversible one-electron reduction of the copper(I) complex. The last reduction process (C) at still more negative potentials is due to the reduction of the free ligand. In case of **13**, a cathodic peak appears at −0.62 V which is likely to be caused by the reduction of the counter-anion $[Cu(NO_3)_4]^{2-}$.

For all complexes the Cu^{2+}/Cu^{+} couple shows reversible character. The ratios of the peak currents (i_{pa}/i_{pc}) are close to unity, and the values of the peak-to-peak separations are comparable with that of the Fc^{+}/Fc couple, although the potential is slightly variable for different complexes with different counter-anions. However, a marked influence on the potentials was found from the solvents in which the cyclic voltammetry experiments were carried out. In dichloromethane, the potentials are anodically shifted, especially significant with OESQ as a pentadentate ligand. The second redox step B is even more sensitive to the experimental conditions, it is expected to result in anion radical ligand species[43] which may decompose to metallic copper and the free ligand. Formation of a metal layer on the electrode is obvious from the copper-dissolving anodic peak (D) in the reverse scan, it can be observed visually on the platinum electrode surface if it is polarised for *ca.* 2 min. at a negative potential. Contrary to the first reduction process, the potentials in dichloromethane are cathodically shifted as

Table 6 Cyclic voltammetry data for complexes of OBSQ[a]

	DMF					CH_2Cl_2	
Compound	$E_{1/2}$[b]	r[c]	E_{pc}[d]	E_{pc}[e]	E_{pc}[f]	$E_{1/2}$[b]	r[c]
15	0.02	1.01	−1.80	−2.41	−2.69	0.43	1.07
16	0.02	1.08	−1.81	−2.42	−2.70	0.47	1.06
17	0.02	0.96	−1.83	−2.43	−2.72	0.39	0.93
18	0.01	1.10	−1.83	−2.44	−2.72	0.33	0.88
19	0.01	1.20	−1.81	−2.42	−2.71	0.15	1.21
21	0.01	1.19	−1.82	−2.43	−2.72	0.40	1.08
23	0.02	0.84	−1.84	−2.46	−2.73	0.49	0.95

[a] Potentials in V *vs.* ferrocenium–ferrocene, 0.1 M Bu_4NPF_6 solutions, platinum working electrode, scan rate 100 mV s^{-1}. The potentials were calculated from the second reference decamethylferrocenium–decamethylferrocene due to overlap of the waves from the complexes and the ferrocenium–ferrocene couple. [b] Half-wave potentials for couple $[Cu^{II}L]^{2+}/[Cu^{I}L]^{+}$. [c] Current ratio i_{pc}/i_{pa}. [d] Cathodic peak potentials for the irreversible $[Cu^{I}L]^{+}/[CuL]^{0}$ reduction step. [e] Cathodic potentials for the irreversible $[CuL]^{0}/[CuL]^{-}$ reduction step. [f] Cathodic peak potentials for the irreversible $[CuL]^{-}/L^{2-}$ reduction step.

compare to those in DMF. The last redox steps C closely resemble the cyclic voltammograms of the free ligands, confirming the product of the second, irreversible reduction process. In dichloromethane, this step is not accessible because of the limited range of the solvent.

As shown in Fig. 10(b) the cyclic voltammograms of the OBSQ complexes exhibit one more cathodic peak as compared with the complexes of OESQ and ODSQ. The reduction of Cu^{2+} to Cu^{+} (A) is reversible at almost the same potential but the second reduction (B) is shifted negatively by about 0.5 V in comparison to the above analogues. The absence of a copper layer on the electrode and copper dissolution processes upon reverse scans suggest that a relatively stable neutral species is produced, in contrast to the result of the second reduction step of OESQ and ODSQ complexes (see also the spectroelectrochemical results below). The neutral species, formally a Cu^{+} complex of an anion radical ligand,[43] may be coupled in a dimeric or polymeric form which could explain the absence of an anodic counterpeak pertinent to the reduction peak B. Accordingly, the third reduction (C) appears at a more negative position than the formation of $OBSQ^{-}$ from free OBSQ, leading to a $[Cu(OBSQ)]^{-}$ species. This negatively charged species can be converted into metallic copper and $OBSQ^{2-}$ by the following reduction step (D) which occurs at a similar potential as the second reduction step of the free OBSQ ligand. Two small anodic peaks, E and F, are related to the reductions C and D; this can be easily confirmed because they will disappear when the scan is cut off before C and D, respectively. The solvent dependence of the $E_{1/2}$ values was again observed, a more cathodic (negative) shift was found in dichloromethane in comparison to the OESQ and ODSQ analogues. An attempt to probe the existence of the neutral $[Cu(OBSQ)]^{0}$ species in CH_2Cl_2 was precluded by the enhanced solvent reduction at negative potentials.

In contrast to the complexes of the OESQ, ODSQ or OBSQ ligands, the redox behaviour of the complexes with the ligands EtSQ and MeSQ differs substantially in different solvents. A wide peak-to-peak separation ($E_{pc} = -0.28$, $E_{pa} = 0.10$ V, $\Delta E_p =$ 380 mV) indicates extensive reorganisation for the Cu^{2+}/Cu^{+} one-electron transfer process in the copper(II) complex **1** in DMF. The ΔE_p value is much smaller at 110 mV in dichloromethane. Similar effects were observed for the copper(I) complexes **2** and **3**, signifying a more extensive structural reorganisation during the electron transfer as evident from structural differences (N–Cu–N angle) and in comparison to the complexes with multidentate ligands.

In general, the complexes described here exhibit more positive potentials for the copper(I/II) couple in comparison to exclusively nitrogen or oxygen donor-coordinated analogues, a result attributed to the incorporation of two sulfur donors atoms.[40a,44] In complexes with the multidentate ligands OESQ, OBSQ and ODSQ, the highest Cu^{2+}/Cu^{+} potentials were found for the complexes of the OBSQ ligand. Since all ligands contain two thioether sulfur donor atoms, an additional contribution apparently comes from the seven-membered chelate ring formed by the *o*-xylylene bridge in comparison to the invariably five-membered rings of other complexes. Such an effect has already been observed and qualitatively explained before[45] and may be a factor for the auto-reduction of the Cu^{2+} complexes mentioned above. The relatively lower potentials for ODSQ complexes compared with OESQ analogues in CH_2Cl_2 solution may be attributed to the replacement of one in-plane sulfur by an oxygen atom. It is known that axially coordinated sulfur atoms have little influence on the redox properties of copper complexes.[22a] However, significant solvent influences on the electrochemistry occur just as was observed for the electronic and EPR spectra. Solvent dependence of $E_{1/2}$ is common for copper complexes, Rorabacher and coworkers have shown that the Cu^{2+}/Cu^{+} potentials are mainly associated with the affinity between the donors and Cu^{2+} ions.[18b,46] The two species detected clearly by EPR for ODSQ and OBSQ complexes in DMF solution cannot be discriminated by cyclic voltammetry, indicating that the equilibrium is faster than the electrochemical response; the Cu^{2+}/Cu^{+} couple observed may just show an average of the structure variations in DMF solution.

In combination with the information obtained from electronic and EPR spectroscopy, the tentative solution structural variations may be summarised as shown in Scheme 2. The

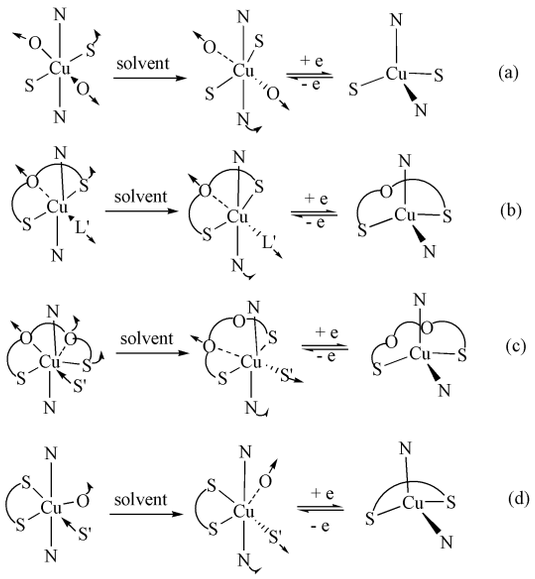

Scheme 2

electrochemically less reversible Cu^{2+}/Cu^{+} couples of complexes **1**–**3** (Scheme 2a) indicate a large structural reorganisation accompanying the electron transfer. The two relatively strong axial Cu^{2+}–O interactions as evident from the crystallographic data may prevent facile rearrangement to the four-coordinate geometry preferred by Cu^{+}, especially in DMF which is a strong coordinating solvent towards Cu^{2+} ions. The situation may get more favourable for the complexes of the OESQ ligand (Scheme 2b). It is known from the structural analyses that the S–Cu–S angle deviates from linearity due to the short diethylene glycol bridge, and the axial O atom interacts only weakly with the Cu^{2+} ion. Therefore, Cu–O bond dissociation may not substantially increase the overall reorganisation energy.[47] A similar situation is present for the ODSQ complexes (Scheme 2c) although dissociation of one equatorial Cu–O bond is necessary. The electronic and EPR spectra showed the existence of such a species which may be stabilised by association with DMF as discussed above. The Cu^{2+} complexes of OBSQ (Scheme 2d) seem to prefer the tetragonal basal geometry, the low $g_{||}$ and $g_{||}A_{||}$ values suggesting only a small degree of tetrahedral distortion. However, the relatively high $E_{1/2}$ values indicate that the ligand OBSQ also satisfies the coordination preference of Cu^{+}.[40a,44] This is supported by the structural analyses where the S–Cu–S angles change little between Cu^{2+} and Cu^{+} complexes, suggesting little structural rearrangement. In addition, only one Cu–O bond of the five-coordinate systems is subject to dissociation, in contrast to the complexes with the other ligands. In conclusion, the good electrochemical reversibility found for all complexes with multidentate ligands suggests facile adjustment of their stereochemistry to accommodate both Cu^{2+} and Cu^{+}, minimising the structural reorganisation during the electron transfer. Such rearrangements may be facilitated by the free Cu–N bond rotation of the two terminal 8-thioquinoline groups. Since the N–Cu–N angles are almost linear in all Cu^{2+} complexes, the structural reorganisation from Cu^{2+} to Cu^{+} complexes can be depicted by a certain degree of rotation of the two sulfur atoms along the N–Cu–N axis, followed by N–Cu–N bending and

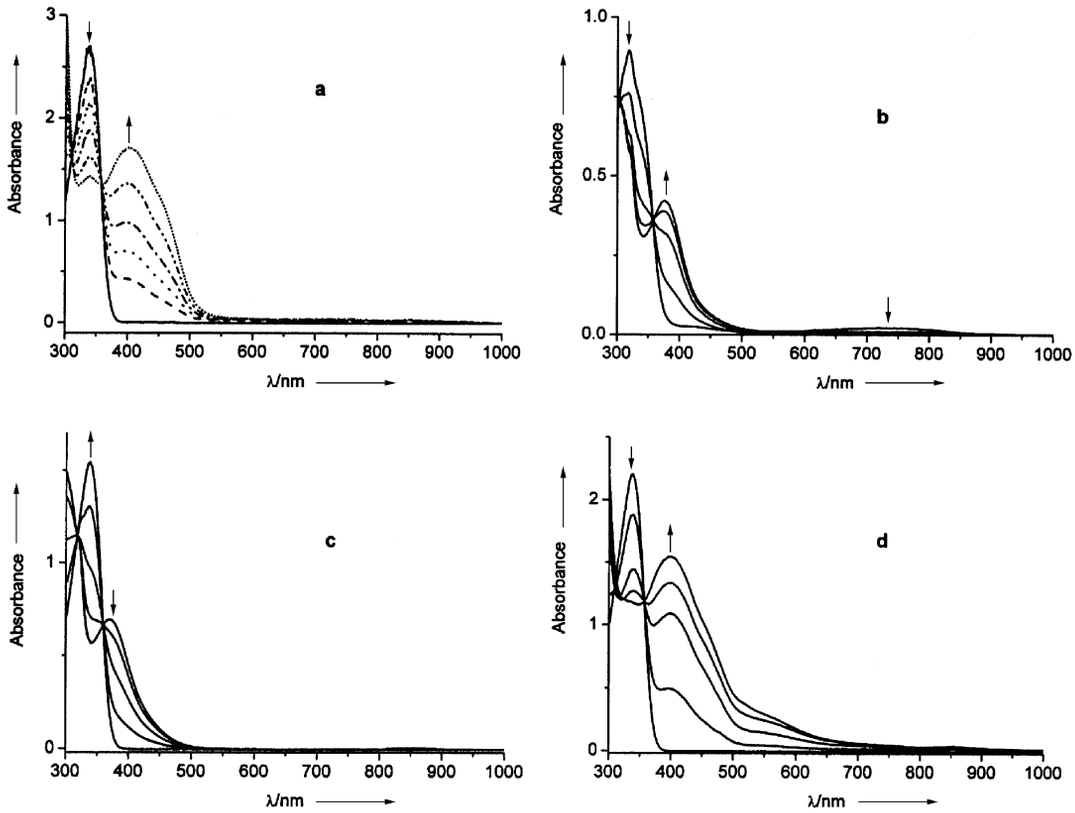

Fig. 11 UV–vis spectroelectrochemistry of (a) the free ligand ODSQ, (b) complex **10** at the first reduction, (c) complex **10** at the second reduction and (d) complex **10** at the third reduction in DMF/0.1 mol dm^{-3} Bu_4NPF_6.

formation of the tetracoordinated complex as shown in Scheme 2.

UV–vis spectroelectrochemistry

An optically transparent thin-layer electrochemical cell[48] was used to investigate the electron transfer behaviour of the compounds **4**, **10** and **17**, representative for each family of complexes with the ligands OESQ, ODSQ and OBSQ. Figs. 11 and 12 depict the UV–vis spectroelectrochemical responses of the free ligands ODSQ and OBSQ together with those of their complexes **10** and **17**, respectively; a figure showing the UV–vis spectroelectrochemical response of complex **4** is provided as ESI (Fig. S7).

In accordance with the results from cyclic voltammetry, the electrolysis at the first reduction peaks of the copper(II) complexes **4** and **10** leads to the disappearance of the weak d–d transitions in the visible and near-infrared regions. In turn, a band due to the copper(I)-based MLCT absorption appears around 370 nm. This obviously indicates that Cu^{2+} is converted to Cu^{+}. On further reduction at the second reduction peak, the MLCT band disappears, and a band at about 337 nm emerges. This band is attributed to the π–π* transition of the free ligand, which shifts to 318 nm after the ligand is coordinated to the Cu^{2+} ion as shown in Fig. 11(a) and (b). This confirms that the free ligand is released after the second reduction and that Cu^{+} is converted to metallic copper. Formation of the free ligand can is also confirmed by subsequent reduction at the third step. A band with a maximum at about 400 nm increases while the π–π* transition band is diminished, almost identical to the behaviour of the free ligand as shown in Fig. 11(a). The spectroelectrochemistry of complexes **4** and **10** is rather similar, therefore, both complexes with the ligands OESQ and ODSQ undergo the same eletrochemical processes as shown in Scheme S2(a) and (b) (ESI).

Complex **17** with the OBSQ ligand exhibits a different spectroelectrochemical response than **4** or **10**. Reduction of Cu^{2+} to Cu^{+} after the first one-electron uptake is clear as shown in Fig. 12(b), and acquisition of one more electron seemingly leads to a similar response as for **4** or **10** as seen from Fig. 12(c). However, subsequent reduction at the third reduction peak does not result in the emergence of a band at ~450 nm as expected from the spectroelectrochemical response of the free ligand OBSQ (Fig. 12(a)), a broad band at ~535 nm appears instead. This finding indicates that the product of the third reduction is not the free ligand anion OBSQ. Attempts to identify multiply reduced species by EPR were not conclusive. Release of the (reduced) ligand is evident only at the last, fourth reduction step during which the broad band at ~535 nm disappears while a band at ~452 nm increases, corresponding to the band as shown in Fig. 12(a) for the reduction of the free ligand OBSQ.

Conclusions

Using the less common 8-alkylthioquinoline imine-S/thioether-S chelate coordination function we have shown that this arrangement is suitable to stabilise both the Cu^{I} and Cu^{II} oxidation states, albeit in structurally different ways than the previously studied mmb ligand. Stronger S and N acceptor and weaker donor effects as well as a smaller N–Cu–S bite are probably responsible for the differences. Coupling of two of these functions by spacers with flexible or semi-rigid backbones with no, one or two additional dialkylether oxygen donor centres for eventual intramolecular coordinative saturation gave a series of complexes for which the solid state structures could be correlated with spectroscopic, cyclic voltammetric and spectroelectrochemical results. The latter include not only the Cu^{I}/Cu^{II} transition but also further reduction processes. In contrast to the simple 8-alkylthioquinolines, MeSQ and EtSQ, the spacer-coupled bis(NS) ligands allow for a more reversible Cu^{I}/Cu^{II} transition due to the various effects of steric constraint (length and flexibility) as imposed by the spacer and due to additional coordination as provided by some of the spacers.

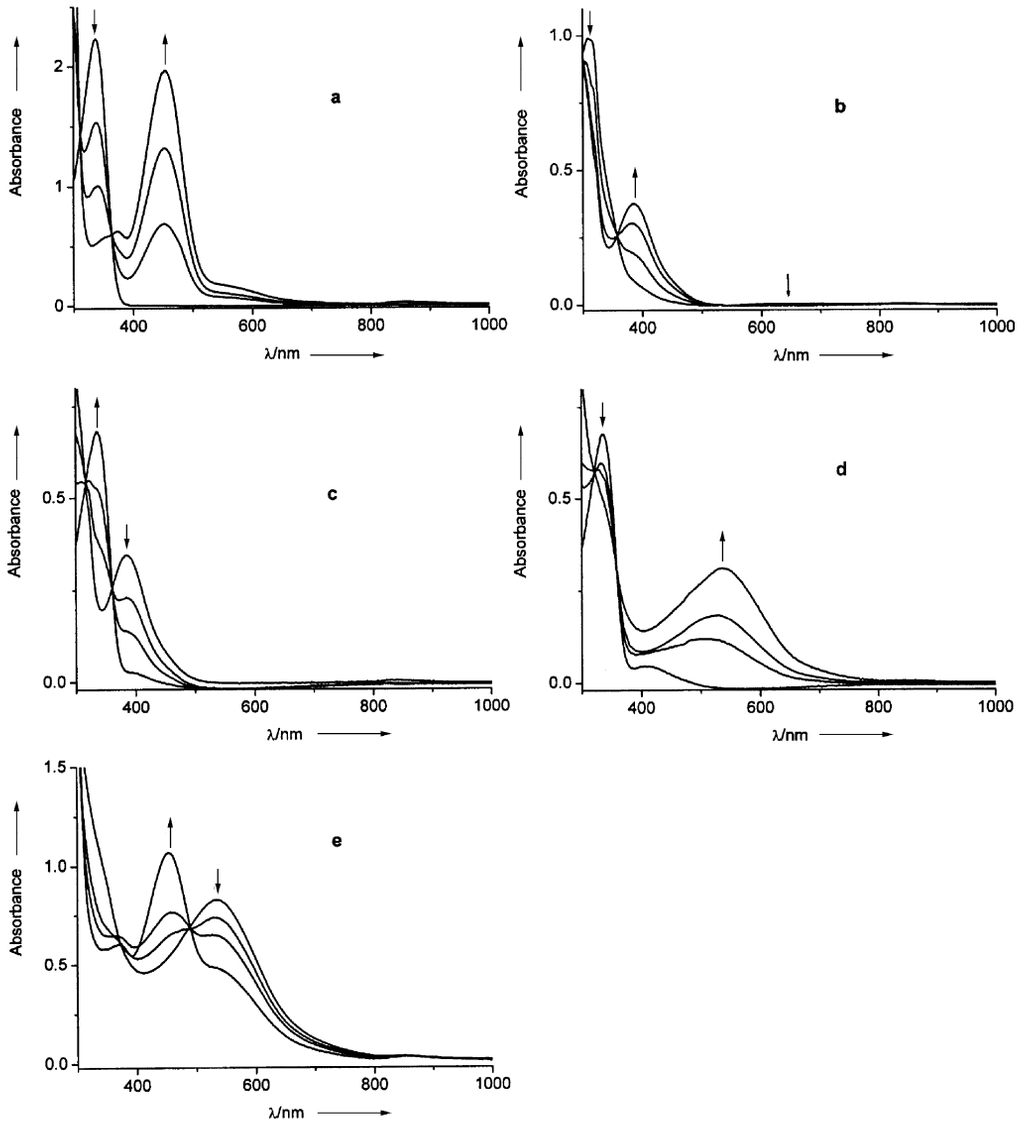

Fig. 12 UV/vis spectroelectrochemistry of (a) the free ligand OBSQ, (b) complex **17** at the first reduction, (c) complex **17** at the second reduction, (d) complex **17** at the third reduction, and (e) complex **17** at the fourth reduction in DMF/0.1 mol dm^{-3} Bu_4NPF_6.

Experimental

General information

Sodium quinoline-8-thiolate was synthesised following a known literature procedure.[10] The ligand 8-methylsulfanylquinoline (MeSQ) was prepared according to the literature.[7] All other reagents and chemicals were purchased from commercial sources.

^{1}H- and ^{13}C-NMR spectra were taken on a Bruker AC 250 spectrometer using $CDCl_3$ as a solvent at room temperature. Infrared spectra were recorded in the range 4000–300 cm^{-1} on a Perkin-Elmer Paragon 1000 PC FTIP instrument using KBr pellets. UV–vis absorption spectra were recorded on a Bruins Instruments Omega 10 spectrophotometer. EPR spectra were measured in the X-band range on a Bruker System ESP 300 equipped with a Bruker ER035M gaussmeter and a HP 5350B microwave counter. Cyclic voltammetry was carried out in solutions containing 0.1 mol dm^{-3} Bu_4NPF_6 using a three-electrode configuration (glassy carbon or platium working electrode, Pt counter-electrode, Ag/AgCl reference) and a PAR 273 potentionstat and function generator. The ferrocene–ferrocenium or decamethylferrocene–decamethylferrocenium couples served the internal references. Spectroelectrochemical measurements were performed using an optically transparent thin-layer electrode (OTTLE) cell[48] for UV–vis spectra. The reversibility of the processes was checked through the appearance of isosbestic points and the restoration of the starting spectra on reoxidation.

Syntheses

1,5-Bis(8-quinolylsulfanyl)-3-oxapentane OESQ. To a mixture of sodium quinoline-8-thiolate (3.7 g, 20 mmol) and KOH (1.2 g, 20 mmol) in 150 mL of absolute EtOH under argon was added dropwise a solution of bis(2-chloroethyl) ether (1.4 g, 10 mmol) in 50 mL of EtOH with vigorous stirring. The reaction mixture was stirred continuously overnight at room temperature. The solvent was removed under reduced pressure. The residue was poured into 100 mL water and extracted three times with dichloromethane (3 × 50 mL). The combined organic extracts were washed with water, dried (Na_2CO_3) and concentrated. The crude product was dissolved in 10 mL ethanol and stored in refrigerator for two days, affording 2.7 g of a white solid. Yield 69%. ^{1}H NMR ($CDCl_3$, ppm) δ 8.96 (dd, 2H, H1, $^2J = 4$, $^3J = 1.5$), 8.15 (dd, 2H, H3, $^2J = 8.0$, $^3J = 1.5$), 7.60 (d, 2H, H5, $^2J = 8.0$), 7.56 (d, 2H, H7, $^2J = 7.0$), 7.48 (dd, 2H, H6,), 7.45 (dd, 2H, H2), 3.85 (t, 4H, H10, ^2J = 7.0), 3.31 (t, 4H, H11, ^2J = 7.0 Hz). ^{13}C NMR ($CDCl_3$, ppm) δ 149.02 (C1), 145.05 (C9), 137.28 (C8), 137.00 (C3), 128.44 (C4), 126.87 (C7), 126.08 (C6), 124.70 (C5), 121.60 (C2), 69.41 (C11), 31.12 (C10). EI-MS, *m/z* (%): 393 (7) [$M^+ + 1$], 188 (70) [$C_9H_6NSCH_2CH_2^+$],

Table 7 Selected bond lengths (Å) and angles (>110°)

Compound	Cu–N	Cu–S	Cu–O	S–Cu–S	N–Cu–N	O–Cu–O	O–Cu–S	N–Cu–S
1	2.024(3)	2.3904(10)	2.425(3)	180.00(4)	180.00(12)	180.00(12)	—	—
3	2.0165(16)	2.3242(6)	—	131.82(10)	117.94(3)	—	—	—
7	1.966(4); 1.972(4)	2.406(2); 2.410(2)	2.113(4); 2.466(4)	147.69(6)	177.7(2)	178.9(2)	—	—
8	1.972(4) 1.978(4)	2.4297(14) 2.4154(14)	2.128(4) 2.519(4)	146.20(6)	177.55(17)	178.55(15	—	—
9	1.994(4) 2.021(4)	2.3707(14) 2.3935(14)	—	128.83(6)	134.77(16)	—	—	—
11	1.994(2) 2.003(2)	2.4099(6) 2.4129(7)	2.271(2) 2.389(2)	130.14(2)	177.18(7)	—	151.09(4) 149.76(4)	—
13	1.992(3) 2.002(3)	2.4031(10) 2.4332(10)	2.265(2) 2.306(2)	127.59(4)	178.57(11)	—	152.04(7) 151.87(6)	—
18·CH_3CN	1.989(4) 2.016(4)	2.3263(15) 2.6155(15)	2.027(3)	—	179.27(15)	—	165.82(9)	—
20	1.993(3) 1.993(3)	2.4882(10) 2.3755(10)	2.023(2)	111.91(3)	173.65(10)	—	152.35(6)	—
21·CH_3CN	1.976(2) 1.982(2)	2.3312(6) 2.5298(6)	2.0212(14)	113.27(2)	177.50(7)	—	161.19(5)	—
22	1.984(3) 1.988(3)	2.3468(9) 2.5140(10)	2.087(3)	116.66(3)	177.48(11)	—	158.83(8)	—
23	1.994(4) 2.013(5)	2.288(2) 2.3173(14)	—	112.29(6)	122.8(2)	—	—	124.39(14) 126.4(2)

160 (36) [$C_9H_6NS^+$], 128 (10) [$C_9H_6N^+$]. IR (KBr, cm^{-1}): $\tilde{\nu}$ = 3059w, 3020w, 2917m, 2858m, 1590m, 1554w, 1490s, 1455s, 1418m, 1357s, 1297m, 1215m, 1116s, 1071w, 1008w, 985s, 818s, 782s, 757m, 657m, 644w, 434w. Elemental analysis: calc. (%) for $C_{22}H_{20}N_2OS_2$: C, 67.32; H, 5.14; N, 7.14; found: C, 67.29; H, 5.02; N, 7.26.

1,8-Bis(8-quinolylsulfanyl)-3,6-dioxaoctane ODSQ. Prepared in a similar way by using 1,2-bis(2-chloroethoxy)ethane instead of bis(2-chloroethyl) ether. Yield 67%. ^{1}H NMR ($CDCl_3$, ppm) δ 8.96 (dd, 2H, H1, ^2J = 4, ^3J = 1.5), 8.14 (dd, 2H, H3, ^2J = 8.0, ^3J = 1.5), 7.59 (d, 2H, H5, ^2J = 8.0), 7.57 (d, 2H, H7, ^2J = 7.0), 7.47 (dd, 2H, H6,), 7.44 (dd, 2H, H2), 3.83 (t, 4H, H10, ^2J = 7.0), 3.67 (s, 4H, H11), 3.32 (t, 4H, H12, ^2J = 7.0 Hz). ^{13}C NMR ($CDCl_3$, ppm) δ 149.00 (C1), 144.93 (C9), 137.51 (C8), 136.96 (C3), 128.50 (C4), 126.96 (C7), 126.30 (C6), 124.74 (C5), 121.63 (C2), 70.44 (C12), 69.70 (C11), 31.12 (C10). EI-MS, *m*/*z* (%): 437 (6) [M^+ + 1]; 276 (20) [$M^+ - C_9H_6NS$], 188 (98) [$C_9H_6NSCH_2CH_2^+$], 160 (46) [$C_9H_6NS^+$], 128 (11) [$C_9H_6N^+$]. IR (KBr, cm^{-1}): $\tilde{\nu}$ = 3053w, 2896m, 2864m, 1597w, 1552w, 1487m, 1452s, 1409m, 1358s, 1289m, 1213m, 1104s, 1071w, 1036m, 985m, 901w, 816m, 788s, 754m, 654w, 549w, 433w. Elemental analysis: calc. (%) for $C_{24}H_{24}N_2O_2S_2$: C, 66.03; H, 5.54; N, 6.42; found: C, 66.23; H, 5.32; N 6.16.

1,2-Bis(quinolin-8-ylsufanylmethyl)benzene OBSQ. To a mixture of sodium quinoline-8-thiolate (3.7 g, 20 mmol) and KOH (1.2 g, 20 mmol) in 100 mL of absolute EtOH under argon was added dropwise a solution of α,α-dibromo-*o*-xylylene (2.6 g, 10 mmol) in 50 mL of EtOH with vigorous stirring. The reaction mixture was stirred continuously for 10 h at 70 °C. After removal of the solvent *in vacuo* the residue was poured into 100 water and extraced with dichloromethane (3 × 50 mL). The combined organic extracts were washed with water, dried (Na_2CO_3) and concentrated. The pale yellow crude product was purified by recrystallisation from CH_2Cl_2–EtOH (1:2, v/v) to give 2.8 g of a colourless crystalline solid. Yield 65%. ^{1}H NMR ($CDCl_3$, ppm) δ 8.95 (dd, 2H, H1, ^2J = 4.3, ^3J = 1.1), 8.16 (dd, 2H, H3, ^2J = 8.2, ^3J = 1.1), 7.87 (d, 2H, H5, ^2J = 8.0), 7.60 (d, 2H, H7, ^2J = 6.1), 7.44 (m, 2H, H2), 7.41 (m, 2H, H6), 7.33 (m, 2H, H13, ^2J = 5.5, ^3J = 3.5), 7.16 (dd, 2H, H12, ^2J = 5.5, ^3J = 3.5 Hz), 4.48 (s, 4H, H10). ^{13}C NMR ($CDCl_3$, ppm) δ 149.36 (C1), 145.24 (C9), 137.76 (C8), 137.71 (C3), 135.35 (C11), 131.07 (C12), 128.73 (C4), 128.20 (C7), 127.57 (C6), 127.35 (C13), 125.31 (C5), 121.93 (C2), 34.70 (C10). IR (KBr, cm^{-1}): $\tilde{\nu}$ = 3056w, 3022w, 1591(m), 1553w, 1489s, 1453m, 1371m, 1299m, 1206w, 985s, 818m, 785s, 749m, 713m, 657m, 463w, 435w, 301w. Elemental analysis: calc. (%) for $C_{26}H_{20}N_2S_2$: C, 73.55; H,4.75; N, 6.60; found: C, 73.59; H, 4.69; N, 6.60.

8-Ethylsulfanylquinoline EtSQ. Prepared in a similar way as OESQ by using sodium quinoline-8-thiolate and iodoethane in an equivalent molar ratio. Yield 50%. ^{1}H NMR ($CDCl_3$, ppm) δ 8.94 (dd, 1H, H1, ^2J = 4.3, ^3J = 1.7), 8.13 (dd, 1H, H3, ^2J = 8.3, ^3J = 1.7), 7.55 (dd, 1H, H5, ^2J = 6.4, ^3J = 3), 7.48 (d, 1H, H7, ^2J = 3), 7.47 (dd, 1H, H6, ^2J = 3), 7.42 (dd, 1H, H2, ^2J = 8.3, ^3J = 4.3), 3.07 (t, 2H, H10, ^2J = 7.4), 1.44 (t, 3H, H11, ^2J = 7.4 Hz). IR (KBr, cm^{-1}): $\tilde{\nu}$ = 3046w, 2967w, 2924w, 1591m, 1556m, 1489s, 1458s, 1362s, 1304m, 1267m, 1220s, 1071w, 987s, 824s, 791m, 765m, 658m, 549w.

General preparation of the complexes. Stoichiometric amounts of metal salt and ligand were dissolved separately in corresponding solvents, and the two resulting solutions were mixed. In most cases, the product precipitated immediately and the mixture was left stand overnight. The product was collected, washed and dried in a desiccator. For copper(I) complexes, degassed solutions were used and the reaction was protected by argon. Detailed syntheses of all the complexes are given as ESI.

X-Ray data collection, structure solution and refinement

Data collection for **1**, **3** and **18**·CH_3CN was performed at −100 °C, and for **7**, **11** and **13** at room temperature on a Siemens P4 four-circle diffractometer with graphite monochromated Mo-Kα radiation (λ = 0.71073 Å) using the ω–2θ scan technique. An empirical absorption correction based on ψ-scans of several reflections was applied. The intensities for **20** were collected at room temperature on a Rigaku AFC5R diffractometer equipped with graphite-monochromated Mo-Kα radiation (λ = 0.71073 Å) from a rotating-anode X-ray generator. Absorption correction was done by the emperical ψ-scan method. The diffraction intensities of **8**, **21**·CH_3CN, **22** and **23** were collected (hemisphere technique) on a Bruker SMART 1K CCD diffractometer, and those of **9** on a NONIUS Kappa CCD diffractometer at ambient temperature. Absorption corrections were performed using the SADABS or HABITUS programs.[49] All structures were solved by direct methods and refined by full-matrix least-squares against F^2 of all data using SHELXTL software.[50] Anisotropic thermal factors were assigned to most of the non-hydrogen atoms with the exceptions of disordered perchlorate anions in **11** and **21**·

CH_3CN, and the tetrafluoroborate anion in **23**. The hydrogen atoms were included in calculated positions (riding model) and refined with fixed $U_{iso} = 1.2U_{iso}$ of the carbon atoms to which they are bonded, except those in **13** and **22** which were included into refinement. The oxygen atoms of the perchlorate anion in **8** were disordered between two slightly different positions and were refined with half site occupancy. One of the perchlorate anions in **11** and both in **21**·CH_3CN exhibited disorder over two locations and were refined with occupancy factors of 0.5. In **23** the disordered tetrafluoroborate anion was refined by setting the free variable as 0.6 for F(1), F(2), F(3) and F(4), and 0.4 for F(1)′, F(2)′, F(3)′ and F(4)′. A summary of crystal data is given in Tables 1 and 2. Selected bond distances and bond angles are listed in Table 7.

CCDC reference numbers 184141–184152.

See http://www.rsc.org/suppdata/dt/b2/b208120m/ for crystallographic data in CIF or other electronic format.

Acknowledgements

We thank the National Natural Science Foundation of China and the Natural Science Foundation of Guangdong Province and the Czech Ministry of Education (grant COST OC D15.10) for financial support. S. C. Y. thanks the Alexander von Humboldt Foundation for a research fellowship. The authors also thank Prof. Thomas C. W. Mak (The Chinese University of Hong Kong), Prof. Albert S. C. Chan (The Hong Kong Polytechnic University), Prof. Kai-Bei Yu (Chinese Academy of Sciences, Chengdu) and Prof. Th. Schleid (Stuttgart University) for assistance with the X-ray diffraction data collection.

References

1 (*a*) E. Ambundo, L. A. Ochrymowycz and D. B. Rorabacher, *Inorg. Chem.*, 2001, **40**, 5133; (*b*) F. Baumann, A. Livoreil, W. Kaim and J.-P. Sauvage, *Chem. Commun.*, 1997, 35; (*c*) M. Albrecht, K. Hübler, S. Zalis and W. Kaim, *Inorg. Chem.*, 2000, **39**, 4731.
2 R. J. P. William, *J. Mol. Catal.–Review Issue*, 1986, 1.
3 (*a*) W. Kaim and J. Rall, *Angew. Chem.*, 1996, **108**, 47; W. Kaim and J. Rall, *Angew. Chem., Int. Ed. Engl.*, 1996, **35**, 43; (*b*) J. A. Guckert, M. D. Lowery and E. I. Solomon, *J. Am. Chem. Soc.*, 1995, **117**, 2817.
4 J. Rall, M. Wanner, M. Albrecht, F. M. Hornung and W. Kaim, *Chem. Eur. J.*, 1999, **5**, 2802.
5 C. G. Pierpont, *Coord. Chem. Rev.*, 2001, **216–217**, 99.
6 (*a*) D. M. Dooley, M. A. McGuirl, D. E. Brown, P. N. Turowski, W. S. McIntire and P. F. Knowles, *Nature (London)*, 1991, **349**, 262; (*b*) C. M. Wilmot, J. Hajdu, M. J. McPherson, P. F. Knowles and S. E. V. Phillips, *Science*, 1999, **286**, 1724.
7 (*a*) E. P. Taylor, *J. Chem. Soc*, 1951, 1150; (*b*) Gialdi and Ponci, *Farm. Ed. Sci.*, 1957, **12**, 194; (*c*) P. Edinger, *Chem. Ber.*, 1908, **41**, 942.
8 (*a*) L. F. Lindoy, S. E. Livingstone and T. N. Lockyer, *Aust. J. Chem.*, 1966, **19**, 1391; (*b*) N. N. Chipanina, D. G. Kim, M. A. Andriyankov, D. D. Taryashinova and G. G. Skvortsova, *Zh. Obshch. Khim.*, 1976, **46**, 1118.
9 L. Pech, Yu. Bankovsky, A. Kemme and A. Sturis, *Latv. Khim. Zh.*, 1991, 392.
10 V. I. Lubenets, N. E. Stadnitskaya and V. P. Novikov, *Russ. J. Org. Chem.*, 2000, **36**, 851; C.-Y. Su, D.-K. Li, W.-Z. Zen and B.-S. Kang, *Acta Sci. Natl. Univ. Sunyatseni*, 1998, **37**, 122.
11 H. Sakamoto, S. Ito and M. Otomo, *Chem. Lett.*, 1995, 37.
12 (*a*) C.-Y. Su, S. Liao, H. L. Zhu, B.-S. Kang, X.-M. Chen and H.-Q. Liu, *J. Chem. Soc., Dalton Trans.*, 2000, 1985; (*b*) S. Liao, C.-Y. Su, C.-H. Yeung, A.-W. Xu, H.-X. Zhang and H.-Q. Liu, *Inorg. Chem. Commun.*, 2000, **3**, 405; (*c*) C.-Y. Su, S. Liao, Y.-P. Cai, C. Zhang, B.-S. Kang and H.-Q. Liu, *Transition Met. Chem.*, 2000, **25**, 593; (*d*) C.-Y. Su, B.-S. Kang, J. Sun, Y.-X. Tong and Z.-N. Chen, *J. Chem. Res. (S)*, 1997, 454.
13 S. Liao, C.-Y. Su, Z.-F. Zhang, H.-Q. Liu and H.-L. Zhu, *Acta Crystallogr. Sect. C*, 2000, **56**, e348.
14 W. T. Carnall, S. Siegel, J. K. Ferrano, B. Tani and E. Gebert, *Inorg. Chem.*, 1973, **12**, 560.
15 S. Kitagawa, M. Munakata and A. Higashi, *Inorg. Chim. Acta*, 1984, **82**, 79.
16 R. Balamurugan, P. Mallayan and R. S. Gopalan, *Inorg. Chem.*, 2001, **40**, 2246.
17 (*a*) L. Casella, M. Gullotti, M. Bartosek, G. Pallanza and E. Laurenti, *J. Chem. Soc., Chem. Commun.*, 1991, 1235; (*b*) F. Champloy, N. Benali-Chéif, P. Bruno, I. Blain, M. Pierrot and M. Réglier, *Inorg. Chem.*, 1998, **37**, 3910; (*c*) T. Ohta, T. Tachiyama, K. Yoshizawa, T. Yamabe, T. Uchida and T. Kitagawa, *Inorg. Chem.*, 2000, **39**, 4358.
18 (*a*) K. K. Nanda, A. W. Addison, R. J. Butcher, M. R. McDevitt, T. N. Rao and E. Sinn, *Inorg. Chem.*, 2000, **39**, 4358; (*b*) E. A. Ambundo, M.-V. Deydier, A. J. Grall, N. Aguera-Vega, L. T. Dressel, T. H. Cooper, M. J. Heeg, L. A. Ochrymowycz and D. B. Rorabacher, *Inorg. Chem.*, 1999, **38**, 4233; (*c*) M. Kodera, T. Kita, I. Miura, N. Nakayama, T. Kawata, K. Kano and S. Hirota, *J. Am. Chem. Soc.*, 2001, **123**, 7715.
19 M. Albrecht, K. Hübler, T. Scheiring and W. Kaim, *Inorg. Chim. Acta*, 1999, **287**, 204.
20 (*a*) R. Bentfeld, N. Ehlers and R. Mattes, *Chem. Ber.*, 1995, **128**, 1199; (*b*) L. R. Hanton, C. Richardson, W. T. Robinson and J. M. Turnbull, *Chem. Commun.*, 2000, 2465; (*c*) P. Comba, A. Fath, G. Huttner and L. Zsolnai, *Chem. Commun.*, 1996, 1885; (*d*) M. R. Malachowski, M. Adams, N. Elia, A. L. Rheingold and R. S. Kelly, *J. Chem. Soc., Dalton Trans.*, 1999, 2177; (*e*) P. Comba, A. Fath, T. W. Hambley and D. T. Richens, *Angew. Chem., Int. Ed. Engl.*, 1995, **34**, 1883.
21 (*a*) M. G. B. Drew, C. Cairns, S. G. McFall and S. M. Nelson, *J. Chem. Soc., Dalton Trans.*, 1980, 2020; (*b*) R. R. Conry, W. S. Striejewske and A. A. Tipton, *Inorg. Chem.*, 1999, **38**, 2833; (*c*) J.-P. Lang, H. Kawaguchi and K. Tatsumi, *Chem. Commun.*, 1999, 2315.
22 (*a*) S. Liu, C. R. Lucas, R. C. Hynes and J.-P. Charland, *Can. J. Chem.*, 1992, **70**, 1773; (*b*) M. J. Prushan, A. W. Addison and R. J. Butcher, *Inorg. Chim. Acta*, 2000, **300**, 992; (*c*) F. Arnaud-Neu, M. J. Schwing-Weill, J. Juillard, R. Louis and R. Weiss, *Inorg. Nuclear Chem. Lett.*, 1978, **14**, 367; (*d*) D. Funkemeier and R. Mattes, *Chem. Ber.*, 1991, **124**, 1357; (*e*) G. Wie, G. G. Allen, T. W. Hambley, G. A. Lawrane and M. Maeder, *Aust. J. Chem.*, 1995, **48**, 825; (*f*) G. Wie, G. G. Allen, T. W. Hambley, G. A. Lawrane and M. Maeder, *J. Chem. Soc., Dalton Trans.*, 1995, 2541.
23 (*a*) C. Keturah, P. A. Tasker and J. Trotter, *J. Chem. Soc., Dalton Trans.*, 1978, 1057; (*b*) S. Pattanayak, P. Chakraborty, S. K. Chandra and A. Chakravorty, *Polyhedron*, 1996, **15**, 1121; (*c*) K. R. Koch, C. Sacht and M. R. Caira, *J. Coord. Chem.*, 1993, **29**, 97.
24 (*a*) E. Bouwman, J. C. T. Hove, W. L. Driessen and J. Reedijk, *Polyhedron*, 1988, **7**, 2591; (*b*) E. Bermejo, R. Carballo, A. Castineiras, A. Lombao, W. Hiller and J. Straehle, *Polyhedron*, 1991, **10**, 1579.
25 A. W. Addison, T. N. Rao, J. Reedijk, J. Van Rijn and G. C. Verschoor, *J. Chem. Soc., Dalton Trans.*, 1984, 1349.
26 A. C. Braithwaite, C. E. F. Rickard and T. N. Waters, *J. Chem. Soc., Dalton Trans.*, 1975, 1817; P. J. M. W. L. Birker, J. Helder, G. Henkel, B. Krebs and J. Reedijk, *Inorg. Chem.*, 1982, **21**, 357; J. van Rijn, W. L. Driessen, J. Reedijk and J.-M. Lehn, *Inorg. Chem.*, 1984, **23**, 3584; P. K. Bharadwaj, J. A. Potenza and H. J. Schugar, *J. Am. Chem. Soc.*, 1986, **108**, 1351; W. G. Haanstra, W. A. J. W. van der Donk, W. L. Driessen, J. Reedijk, M. G. B. Drew and J. S. Wood, *Inorg. Chim. Acta*, 1990, **176**, 299; E. Bouwman, R. Day, W. L. Driessen, W. Tremel, B. Krebs, J. S. Wood and J. Reedijk, *Inorg. Chem.*, 1988, **27**, 4614; N. Goswami and D. M. Eichhorn, *Inorg. Chim. Acta*, 2000, **303**, 271; K. D. Karlin, P. L. Dahlstrom, J. R. Hyde and J. Zubieta, *Chem. Commun.*, 1980, 906; R. P. Hauser and W. B. Tolman, *Inorg. Chem.*, 1995, **34**, 1632.
27 (*a*) G. E. Norris, B. F. Anderson and E. N. Baker, *J. Am. Chem. Soc.*, 1986, **108**, 2784; (*b*) E. N. Baker, *J. Mol. Biol.*, 1988, **203**, 1071; (*c*) H. Nar, A. Messerschmidt, R. Huber, M. Vandekamp and G. W. Canters, *J. Mol. Biol.*, 1988, **203**, 1071.
28 (*a*) N. Aoi, G.-E. Matsubayashi and T. Tanaka, *J. Chem. Soc., Dalton Trans.*, 1983, 1059; (*b*) V. B. Pett, L. L. Diaddario Junior, E. R. Dockal, P. W. Corfield, C. Ceccarelli, M. D. Glick, L. A. Ochrymowycz and D. B. Rorabacher, *Inorg. Chem.*, 1983, **22**, 3661; (*c*) I. L. Karle, D. Ranganathan and S. Kurur, *J. Am. Chem. Soc.*, 1999, **121**, 7156.
29 (*a*) A. B. P. Lever, *Inorganic Electronic Spectroscopy*, Elsevier, 2nd edn., 1984, p. 554; (*b*) B. J. Hataway and A. A. G. Tomlinson, *Coord. Chem. Rev.*, 1970, **5**, 1; (*c*) B. J. Hataway, M. Duggan, A. Murphy, J. Mullane, C. Power, A. Walsh and B. Walsh, *Coord. Chem. Rev.*, 1981, **36**, 267.
30 I. Persson, P. Persson, M. Sandström and A.-S. Ullström, *J. Chem. Soc., Dalton Trans.*, 2002, 1256.
31 A. B. P. Lever and E. Mantovani, *Inorg. Chem.*, 1971, **10**, 817.
32 (*a*) G. A. McLachlan, G. D. Fallon, R. L. Martin and L. Spiccia, *Inorg. Chem.*, 1995, **34**, 254; (*b*) M. Murali, M. Palaniandavar and

T. Pandiyan, *Inorg. Chim. Acta*, 1994, **224**, 19; (*c*) F. A. Chavez, M. M. Olmstead and P. K. Mascharak, *Inorg. Chem.*, 1996, **35**, 1410; (*d*) L. Antolini, G. Marcotrigiano, L. Menabue and G. C. Pellacani, *J. Am. Chem. Soc.*, 1980, **102**, 1303; (*e*) S. Tyagi and B. J. Hathaway, *J. Chem. Soc., Dalton Trans.*, 1983, 199.
33 P. Comba, A. Fath, T. W. Hambley and A. Vielfort, *J. Chem. Soc., Dalton Trans.*, 1997, 1691.
34 (*a*) E. I. Solomon, M. J. Baldwin and M. D. H. Lowery, *Chem. Rev.*, 1992, **92**, 521; (*b*) H. Yokoi and H. W. Addison, *Inorg. Chem.*, 1977, **16**, 1341; (*c*) A. W. Addison and E. Sinn, *Inorg. Chem.*, 1988, **22**, 1225; (*d*) B. J. Hathaway, in *Comprehensive Coordination Chemistry*, vol. 5 (ed. G. Wilkinson), Pergamon, Oxford, 1987, p. 533.
35 (*a*) R. P. F. Kanters, R. Yu and A. W. Addison, *Inorg. Chim. Acta*, 1992, **196**, 97; (*b*) J. V. Dagdigian, V. McKee and C. A. Reed, *Inorg. Chem.*, 1982, **21**, 1332; (*c*) V. M. Miskowski, J. A. Thich, R. Solomon and H. J. Schugar, *J. Am. Chem. Soc.*, 1976, **98**, 8344; (*d*) M. Vaidyanathan, R. Balamurugan, U. Sivagnanam and M. Palaniandavar, *J. Chem. Soc., Dalton Trans.*, 2001, 3498.
36 (*a*) M. Melnik, *Coord. Chem. Rev.*, 1981, **36**, 1; (*b*) F. A. Walker, H. Sigel and D. B. McCormick, *Inorg. Chem.*, 1972, **11**, 2756.
37 (*a*) A. J. Blake, J. P. Danks, I. A. Fallis, A. Harrison, W.-S. Li, S. Parsons, S. A. Ross, G. Whittaker and M. Schröder, *J. Chem. Soc., Dalton Trans.*, 1998, 3969; (*b*) J. Peisach and W. E. Blumberg, *Arch. Biochem. Biophys.*, 1974, **165**, 691.
38 A. W. Addison, in *Copper Coordination Chemistry: Biochemical, Inorgani. Perspectives*, ed. K. D. Karlin and J. Zubieta, Adenine Press, New York, 1983, pp. 111.
39 (*a*) G. R. Brubaker, J. N. Brown, M. K. Yoo, R. A. Kinsey, T. M. Kutchan and E. A. Mottel, *Inorg. Chem.*, 1979, **18**, 299; (*b*) Y. Sunatsuki, T. Matsumoto, Y. Fukushima, M. Mimura, M. Hirohata, N. Matsumoto and F. Kai, *Polyhedron*, 1998, **17**, 1943; (*c*) T. M. Donlevy, T. W. Gahan, G. R. Hanson, K. L. McMahon and R. Stranger, *Inorg. Chem.*, 1994, **33**, 5131.
40 (*a*) A. W. Addison, *Inorg. Chim. Acta*, 1989, **162**, 217; (*b*) E. V. Rybak-Akimova, A. Y. Nazarenko, L. Chen, P. W. Krieger, A. M. Herrera, V. V. Tarasov and P. D. Robinson, *Inorg. Chim. Acta*, 2001, **324**, 1.
41 A. S. Silva, M. A. A. de Silva, C. E. M. Carvalho, O. A. C. Antunes, J. O. M. Herrera, I. M. Brinn and A. S. Mangrich, *Inorg. Chim. Acta*, 1999, **292**, 1.
42 (*a*) M. J. Schilstra, P. J. M. W. L. Birker, G. C. Verschoor and J. Reedijk, *Inorg. Chem.*, 1982, **21**, 2637; (*b*) B. Adhikary and C. R. Lucas, *Inorg. Chem.*, 1994, **33**, 1376; (*c*) R. Balamurugan, M. Palaniandavar and R. S. Gopalan, *Inorg. Chem.*, 2001, **40**, 2246.
43 A. F. Stange, E. Waldhör, M. Moscherosch and W. Kaim, *Z. Naturforsch., Teil B*, 1995, **50**, 115.
44 (*a*) J. G. Gilbert, A. W. Addison, A. Y. Nazarenko and R. J. Butcher, *Inorg. Chim. Acta*, 2001, **324**, 123; (*b*) G. S. Patterson and R. H. Holm, *Bioinorg. Chem.*, 1975, **4**, 257.
45 D. E. Nickles, M. J. Powers and F. L. Urbach, *Inorg. Chem.*, 1983, **22**, 3210.
46 (*a*) E. R. Dockal, T. E. Jones, W. F. Sokol, R. J. Engerer, D. B. Rorabacher and L. A. Ochrymowycz, *J. Am. Chem. Soc.*, 1972, **98**, 4322; (*b*) M. M. Bernardo, M. J. Heeg, R. R. Schroeder, L. A. Ochrymowycz and D. B. Rorabacher, *Inorg. Chem.*, 1992, **31**, 191.
47 K. Krylova, C. P. Kulatilleke, M. J. Heeg, C. A. Salhi, L. A. Ochrymowycz and D. B. Rorabacher, *Inorg. Chem.*, 1999, **38**, 4322.
48 M. Krejcik, M. Danek and F. Hartl, *J. Electroanal. Chem.*, 1991, **317**, 179.
49 (*a*) G. M. Sheldrick, SADABS. Program for scalling and correction of area detector data, University of Göttingen, Göttingen, Germany, 1996; (*b*) W. Herrendorf, HABITUS, Programm zur Optimierung der Kristallgestalt für die numerische Absorptionskorrektur, Dissertation, Universität Karlsruhe, Germany, 1993.
50 SHELXTL, Version 5.10, Bruker Analytical X-ray Systems, Madison, WI, 1998.